



climate change initiative

European Space Agency

Climate Research Data Package (CRDP) - Technical Document Phase 2 Year 3



glaciers
cci

Prepared by: Glaciers_cci consortium
Contract: 4000109873/14/I-NB
Name: Glaciers_cci-D4.2_CRDP-TD
Version: 1.1
Date: 12.05. 2018

Contact:
Frank Paul
Department of Geography
University of Zurich
frank.paul@geo.uzh.ch

Technical Officer:
Stephen Plummer
ESA ESRIN



UNIVERSITY
OF OSLO



University of
Zurich^{UZH}



UNIVERSITY OF LEEDS

 **GAMMA REMOTE SENSING**



Document status sheet

Version	Date	Changes	Approval
0.1	23.01. 2015	Initial draft	
0.2	04.04. 2015	Extended draft with examples for all sections	
0.3	20.04. 2015	Contributions from consortium partners integrated	
0.4	14.05. 2015	Further contributions from partners integrated	
0.5	16.06. 2015	Comments from the TO integrated	F. Paul
0.6	16.02. 2016	Initial year 2 update	
0.7	30.05. 2016	All datasets created in year 2 included	F. Paul
0.8	17.08. 2016	Comments from TO integrated	
0.9	11.11. 2017	Initial year 3 update	F. Paul
1.0	21.12. 2017	Comments from TO integrated	
1.1	18.05. 2018	Final datasets integrated and described	

The work described in this report was done under ESA contract 4000109873/14/I-NB. Responsibility for the contents resides with the authors that prepared it.

Author team:

Frank Paul, Philipp Rastner, Nico Mölg, Tobias Bolch (GIUZ), Christopher Nuth, Robert McNabb, Andreas Käab (GUIO), Thomas Nagler, Gabriele Schwaizer, Jan Wuite (ENVEO), Kate Briggs, Andrew Shepherd, (SEEL), Tazio Strozzi (Gamma)

Glaciers_cci Technical Officer at ESA:
Stephen Plummer

Table of Contents

Document status sheet	2
Table of Contents	3
1. Purpose of this document.....	4
2. Accessing the Climate Research Data Package	5
3. Data products overview	8
4. Glacier area	9
4.1 Western Greenland	9
4.2 Novaya Zemlya	10
4.3 Franz-Josef-Land	11
4.4 European Alps	12
4.5 Patagonia	13
4.6 South Georgia	14
5. Elevation Change (ALT).....	15
5.1 Greenland (peripheral glaciers).....	15
6. Elevation Change (DEM).....	16
6.1 Greenland	16
6.2 Svalbard	17
6.3 Caucasus	18
7. Velocity	20
7.1 Greenland	20
7.2 Svalbard	22
7.3 Circum-Arctic glaciers	23
7.4 Karakoram	28
7.5 Patagonia	30
7.6 South Georgia	31
7.7 Alexander Island, Antarctic Peninsula	32
8. Phase 2 data production overview	33
References	34
Abbreviations	35

1. Purpose of this document

This is a technical document describing the contents of the Climate Research Data Package (CRDP) of the Glaciers_cci project in year 3 of Phase 2. It provides for all datasets created a short description, an overview map showing what the datasets look like and tabular information on the satellite scenes used (sections 4-7). More details for all datasets can be found on the respective 'metadata information sheets' provided along with the dataset. The overview section (3) presents all datasets in tabular format along with the related RGI region. The CRDP itself is provided on a separate webpage (<http://glaciers-cci.enveo.at>) containing zip files along with the respective metadata for each product and dataset (see Section 2). An overview presenting all datasets created in Phase 2 is provided in section 8.

2. Accessing the Climate Research Data Package

The products generated within Glaciers_cci are stored in the Climate Research Data Package (CRDP), which can be accessed after registration via the website <http://glaciers-cci.enveo.at>. The tab CRDP in the menu bar links to an introduction of the CRDP, and provides a direct link to access the database (Fig. 2.1).

Each of the datasets contains a metadata description with meta-information on the content of the file, product version, generation date, institute and author, satellite data used as input, geographical coverage, etc.



Fig. 2.1: CRDP access on the website <http://glaciers-cci.enveo.at>.

Accessing products

There is a two-step procedure for accessing the database, related to (i) viewing and selecting of products and (ii) downloading the products. The first step “Viewing and selecting does not require any registration. In the second step “Downloading of the product” we ask for the approval of a data usage disclaimer by providing name, affiliation and email address, a password is not required (see Figure 2.2). The entered information is used only for tracking the use of the products.

GLACIER CCI CRDP Disclaimer

DATA USE AND COPYRIGHT

You may download and use any products from this web site, but please recognize the stated limitations for its use. All datasets are provided by the ESA Glaciers_cci consortium.

WHY CITE ESA GLACIERS_CCI DATA SETS?

A citation acknowledges our data contributors, and allows us to track the use and impact of our data. It also helps us report data distribution to funding agencies, and to assist others who may contact us about data that are referenced in publications.

HOW TO CITE ESA GLACIERS_CCI DATA

Please include a citation in the acknowledgement section of your work: The dataset [data set name] used here was provided by ESA Glaciers_cci. When a product-related publication is listed in the metadata sheets attached to each product, please cite it in the references section of your publication.

LOGIN

To help us keep track of data downloads, please sign in below with your name, institution and email address, or with your Facebook or Google account:

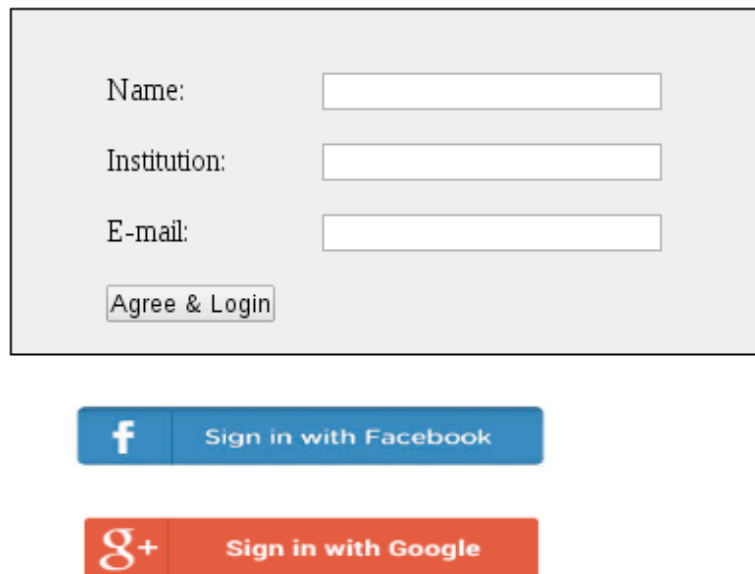


Fig. 2.2: Data disclaimer and login screen for accessing the database.

Entering the Glaciers_cci CRDP database provides direct access to the generated products. Figure 2.3 shows screenshots of the four main panels in the CRDP database: glacier area, elevation change (altimetry), elevation change (DEM differencing), and ice velocity. Further datasets will be added as they become available. Details of new datasets are provided in the following sections of this document.

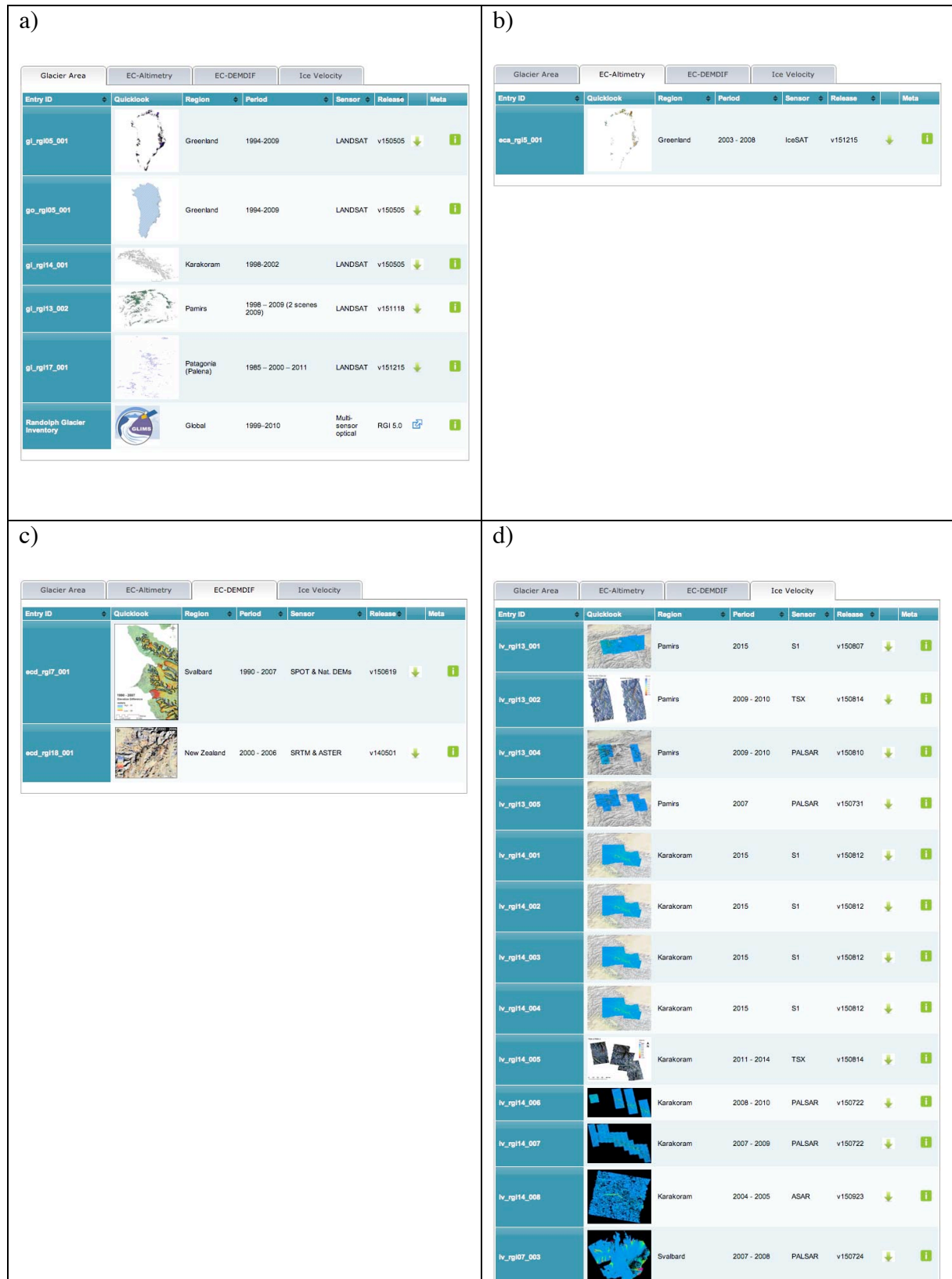


Figure 2.3: Screenshots of the four main panels of the CRDP database: a) glacier area, b) EC-altimetry, c) EC-DEMDIF, and d) ice velocity. All datasets are publicly available after providing basic registration info. xxx **update**

3. Data products overview

In Table 3.1 we provide an overview of the products generated in year 3 of Phase 2. Regions were selected based on user requirements (e.g. improvement of RGI outlines), the work suggested in the technical proposal (e.g. change assessment), or specific science needs (e.g. the pan-Arctic dataset). Some glacier outlines have already been forwarded to the RGI / GLIMS for database ingest (e.g. Nr. 2) or were made available on the server. Please note: RGI regions (see Fig. 3.1) are only given for orientation, they are not necessarily completely covered.

Nr.	Region	RGI#	Satellite	Products	Period	Ch.
1	Western Greenland	5	Landsat 8, Sentinel 2	Area (Inventory)	2016	4.1
2	Novaya Zemlya	9	Landsat 8	Area (Inventory)	2013-16	4.2
3	Euopean Alps	11	Sentinel 2	Area (Inventory)	2015-17	4.3
4	Patagonia	17	Landsat 8	Area (Inventory)	2016	4.4
5	South Georgia	19	Landsat 8	Area (Inventory)	2016	4.5
6	Greenland (periph.)	14	Cryosat-2	Elev. Change (Altimetry)	2010-14	5.1
7	Northern Greenland	5	AeroDEM/ArcticDEM	Elev. Change (dDEM)	1978-2014	6.1
8	Svalbard	6	nat./SPOT/TanDEM-X	Elev. Change (dDEM)	var.-2014	6.2
9	Caucasus	12	SRTM/ASTER	Elev. Change (dDEM)	2000-2015	6.3
10	Greenland (periph.)	5	Sentinel 1	Velocity (SAR)	2014/15/16	7.1
11	Svalbard	7	Sentinel 1	Velocity (SAR)	2015/16	7.2
12	Circum Arctic	13	Palsar, S1, TSX	Velocity (SAR)	2 periods	7.3
14	Karakoram	14	Sentinel 1, Landsat 7/8	Velocity time series	2013-16	7.4
13	Patagonia	17	Sentinel 1	Velocity (SAR)	2015	7.5
15	South Georgia	19	Sentinel 1	Velocity (SAR)	2015	7.6
16	Alexander Island	19	Sentinel 1	Velocity (SAR)	2015	7.7

Table 3.1: Overview of the generated products in each RGI region (see numbers in Fig. 3.1).

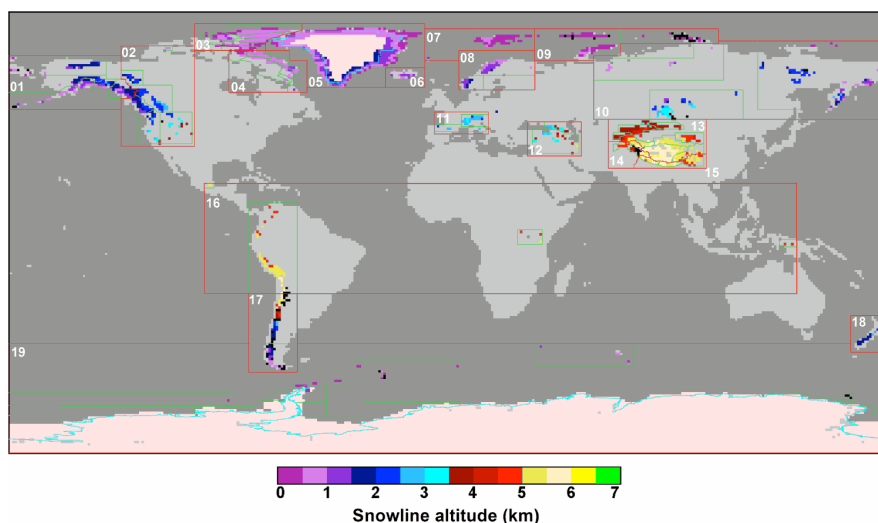
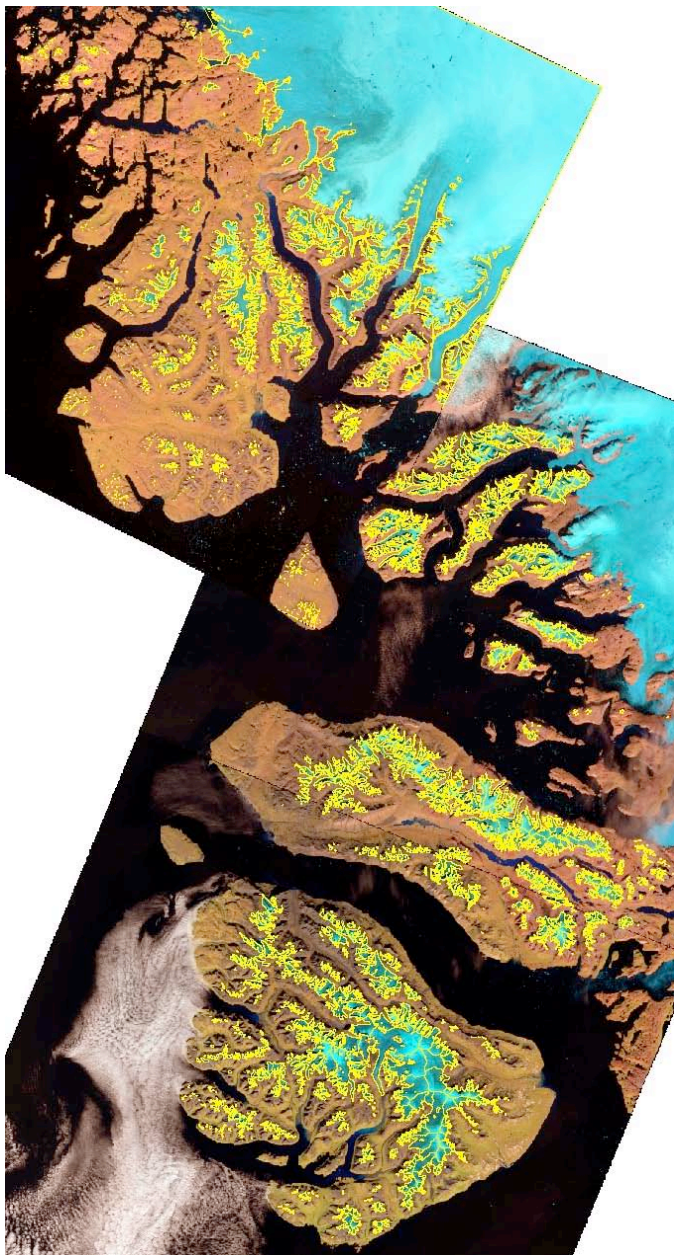


Figure 3.1: Overview of the subregions in the RGI with colour-coded median elevations of the glacierized regions (from Arendt et al. 2015).

4. Glacier area

Data production in year 3 focused on creating up-to-date glacier outlines for peripheral glaciers on central western Greenland, Novaya Zrmlya, the Alps and Patagonia using latest Sentinel 2 and Landsat 8 data. For some regions (Patagonia, South Georgia) we have also created historic outlines (around the year 2000) to replace poor quality outlines in the current RGI. The individual sections below provide quicklooks of the new datasets for each region along with an overview of source data used and/or important references.

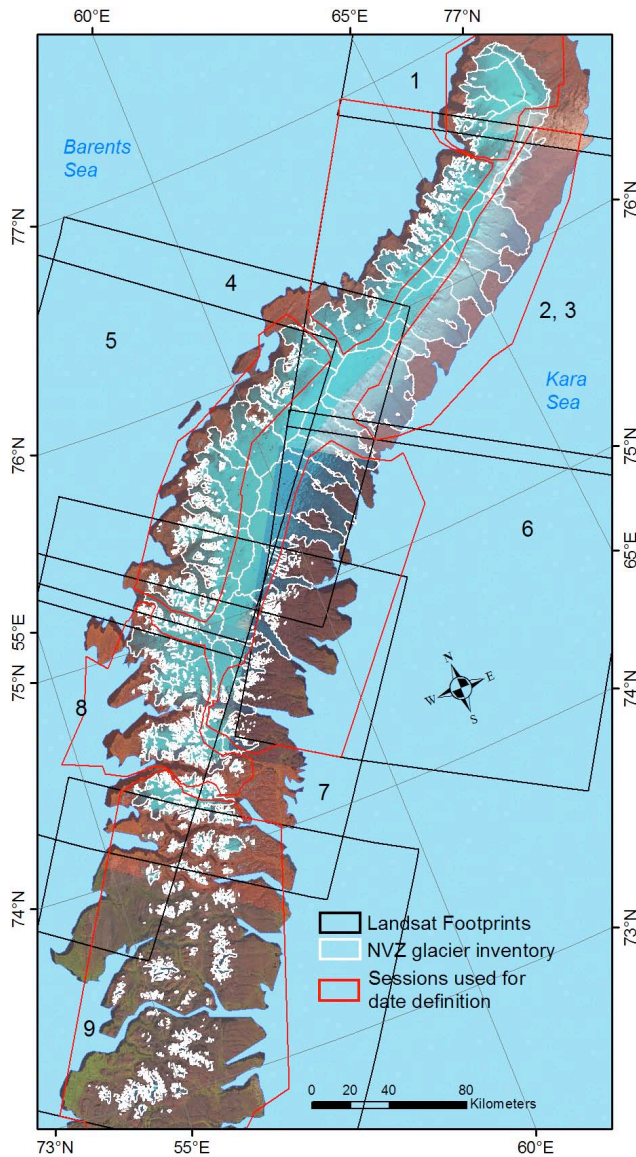
4.1 Western Greenland



For central western Greenland (Disko Island, Nuussuaq and Svartenhuuk Peninsula) we have created new glacier outlines from Landsat 8 OLI data acquired on 1.8. 2015 (scene 15-09) and 30.8.2016 (scenes 12-10/11). The three scenes are shown along with the generated glacier outlines in Fig. 4.1. Sentinel 2 scenes from August 2017 have been used to support identification of rock glaciers and ice-debris features, partly resulting in a different interpretation of glacier extents than in the previous inventory from 2001 (Citterio et al. 2009). The TanDEM-X DEM (DLR Proposal DEM_GLAC0606) has been used to derive new drainage divides and for calculation of topographic information for each glacier.

Fig. 4.1: The new glacier inventory for central western Greenland (yellow outlines) are shown on top of the three satellite images used to create the inventory).

4.2 Novaya Zemlya



New glacier outlines have been created for Novaya Zemlya in the Russian Arctic (Fig. 4.2) from seven Landsat 8 scenes (see Table 4.2) acquired in 2013, 2015 and 2016. In a region with abundant seasonal snow, two Landsat TM scenes from 1998 were used for the initial mapping and two scenes from 2015 were used to adjust glacier terminus positions. The ArcticDEM (5 m resolution) was used after void filling with the ASTER GDEM2 to derive drainage divides and topographic information for each glacier. Fringes from SAR data were used to further refine the location of drainage divides in the accumulation region. The publication by [Rastner et al. \(2017\)](#) provides further details.

Fig. 4.2: The new glacier inventory for Novaya Zemlya (outlines in yellow) and the footprints of the Landsat scenes (black) used to create outlines (see Table 4.2). A selection of the satellite scenes used is shown in the background.

Nr.	Sensor	Path-Row	Date	Comments
1	OLI	176/005	2013 08 19	raw mapping
2	OLI	176/006	2015 09 10	cloud covered E
3	OLI	176/006	2013 08 19	cloud covered W
4	OLI	180/006	2015 08 05	front position update
5	OLI	181/006	1998 08 29	raw mapping
6	OLI	176/007	2013 08 03	raw mapping
7	OLI	179/007	2015 07 29	front position update
8	TM	181/007	1998 08 29	raw mapping
9	OLI	178/008	2016 08 10	raw mapping

Table 4.1: Overview of the processed Landsat scenes used to derive the glacier outlines.

4.3 Franz-Josef-Land

A new glacier inventory has been created for Franz-Josef Land (Russian Arctic) from Sentinel 2 images that have mostly been acquired on 12.9.2016 (Table 4.2) and the new ArcticDEM to derive drainage divides (Fig. 4.3) and topographic parameters. Four tiles (nr. 6, 8, 10, 11) from July 2016 were used to fill data gaps (e.g. due to clouds). From the ArcticDEM 25 5 m resolution mosaic tiles were used. They had only few and small data voids that had been filled with data from a co-registered ASTER GDEM2. The location of drainage divides is partly considerably shifted compared to the RGI and strong retreat of most marine terminating glacier can be seen (Fig. 4.3, inset).

Nr.	Scene	Date	Nr.	Scene	Date	Nr.	Scene	Date
1	38XNQ	2016 09 12	5	40XDR	2016 09 12	9	40XEP	2016 09 12
2	39XVL	2016 09 12	6	40XER	2016 07 12	10	40XDQ	2016 07 10
3	39XVJ	2016 09 12	7	40XEQ	2016 09 12	11	41XNK	2016 07 06
4	39XWK	2016 09 12	8	40XEP	2016 07 14	12	41XNK	2016 09 12

Table 4.2: Overview of the processed Sentinel 2 scenes used to derive the glacier outlines.

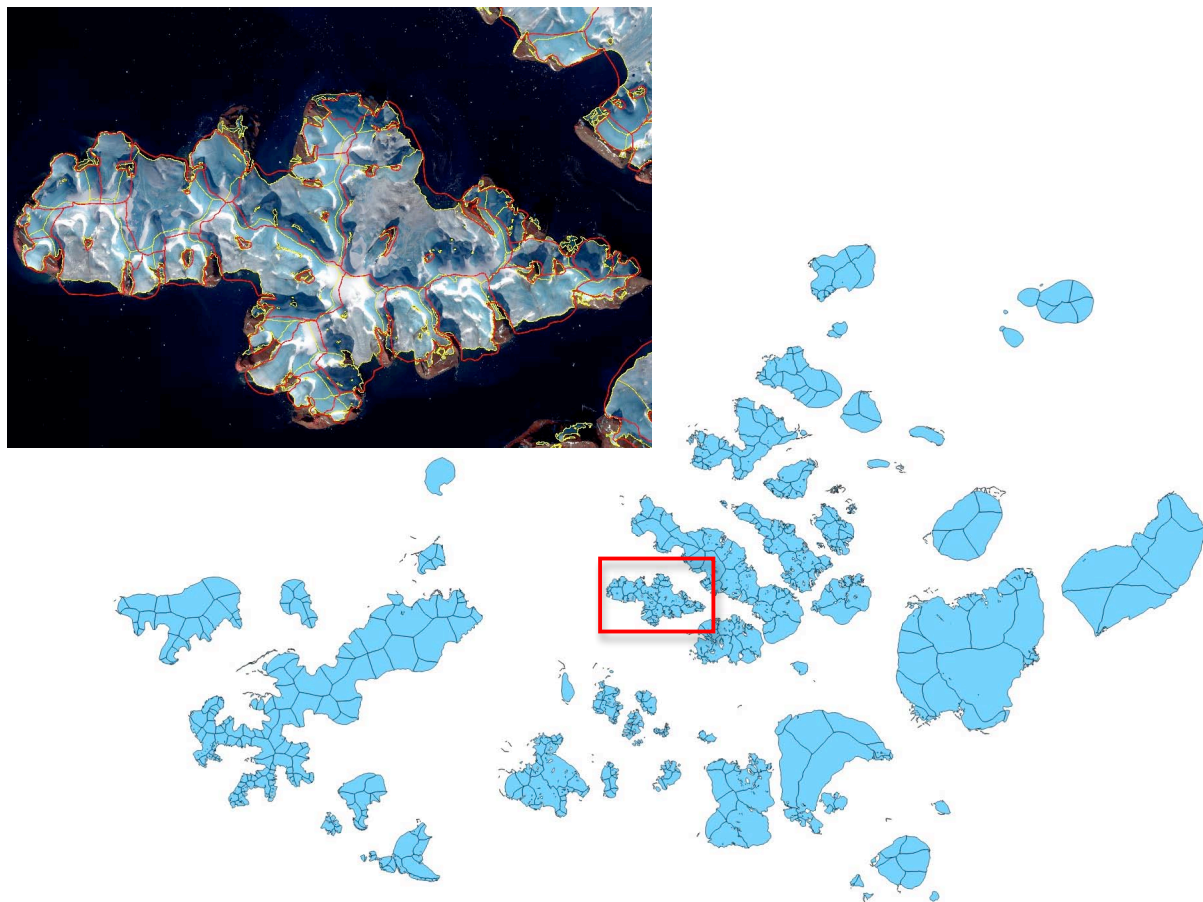


Fig. 4.3: The large image shows the new outlines and ice divides generated for Franz-Josef-Land from Sentinel 2 scenes of 2016 and the ArcticDEM. The smaller inset shows the new outlines (yellow) along with the RGI outlines (red) as an overlay on the Sentinel 2 image for Luigi Island (red square).

4.4 European Alps

A new glacier inventory for the entire European Alps has been created from Sentinel 2 scenes acquired in August 2015 for most of the study region. Due to orographic clouds in the south, outlines for Italy had to be derived from scenes of another date (September 2016) or sensor (Landsat OLI from 2017). The work was performed together with colleagues from France, Italy and Austria who performed the corrections in their country considering the outlines from their latest national inventories as a guide. Drainage divides were also copied from these former inventories but topographic information for each glacier are mostly derived from the TanDEM-X DEM. The satellite scenes used are listed in Table 4.3 and Fig. 4.3 presents an overview of the available Sentinel 2 scenes from August 2015. Additional tiles from 2016 are used to map glaciers in Italy as they suffer from cloud cover in 2015.

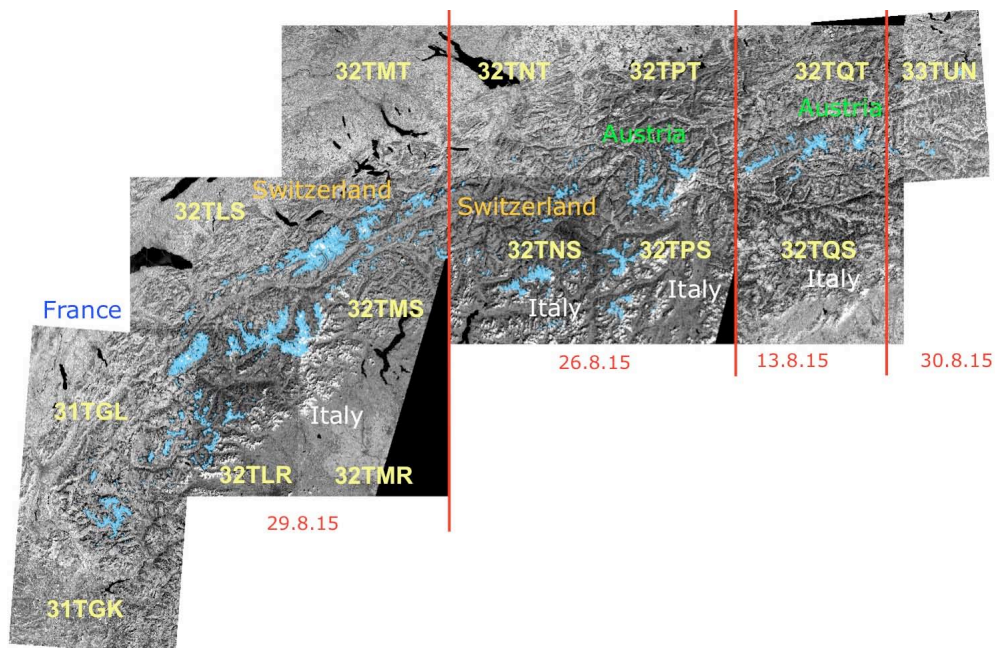


Fig. 4.3: Glacier outlines (light blue) on top of the Sentinel 2 tiles (band 8 in the near infrared) used for glacier mapping in 2015. Some additional scenes are listed in Table 4.3.

Nr.	Scene	Date	Country	Nr.	Scene	Date	Country
1	31TGL	2015 08 29	FR	10	32TNS	2015 08 26	CH
2	31TGK	2015 08 29	FR	11	32TNS	2016 09 16	IT
3	32TLS	2015 08 29	CH	12	32TPT	2015 08 26	AU
4	32TLR	2015 08 05	CH/IT	13	32TPS	2016 08 26	AU
5	32TLQ	2015 08 29	IT	14	32TPS	2016 09 16	IT
6	32TMT	2015 08 29	CH	15	32TQT	2015 08 13	AU/IT*
7	32TMS	2015 08 29	CH/IT	16	32TQS	2016 08 07	IT
8	32TMR	2015 08 29	CH/IT	17	33TUN	2015 08 30	AU
9	32TNT	2015 08 26		18	33TUM	2016 08 27	IT

Table 4.3: Satellite scenes from Sentinel 2 that have been used to create the new glacier inventory for the Alps. *For the Italian part of scene 32TQT a Landsat 8 scene (192-027) from 30.8. 2017 has been used for glacier mapping.

4.5 Patagonia

For all of Patagonia we created a new glacier inventory from eight Landsat 8 scenes acquired in March 2016 and two scenes from 2013 (see Table 4.4). An additional Landsat 5 TM scene from 2011 was used for mapping glaciers covered by clouds in scene Nr. 10. Drainage divides and topographic information were derived from the TanDEM-X DEM (resampled to 30 m_merged with the ASTER GDEMv2 in regions with data voids). Figure 4.4 shows the related glacier outlines (colour-coded by scene) before they were merged

Nr.	Path-Row	Date	Day	Nr.	Path-Row	Date	Day	Comment
1	232-089	2016 03 12	72	8	231-093	2016 03 05	65	some clouds
2	232-090	2016 03 12	72	9	231-094	2016 03 05	65	some clouds
3	232-091	2016 03 12	72	10	231-095	2016 02 02	33	some clouds
4	232-092	2016 03 12	72	11	231-095	2011 02 21	51	Landsat 5 TM
5	232-093	2016 03 12	72	12	230-096	2013 04 23	113	deep shadows
6	232-094	2016 03 12	72	13	230-097	2013 04 23	113	deep shadows
7	232-095	2016 03 12	72	14				

Table 4.4: Satellite scenes from Sentinel 2 MSI that have been used to create the new glacier inventory for the Alps. For the Italian part a Landsat 8 OLI scene (192-027) from 30.8. 2017 has been used for glacier mapping.

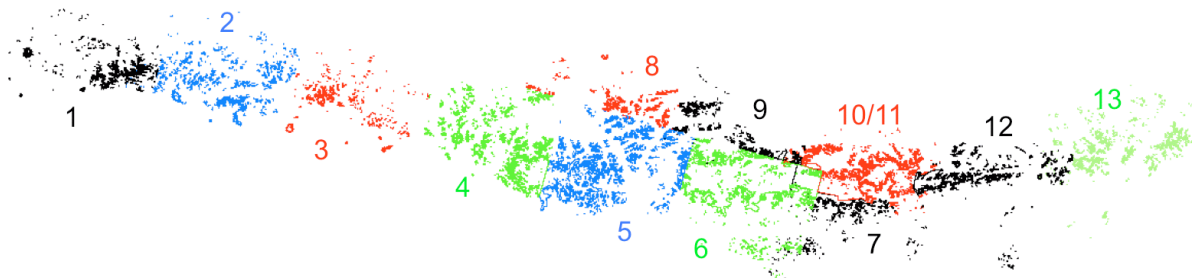


Fig. 4.4: Glacier outlines for the new inventory of Patagonia for the year 2016 (scenes 1-10) and 2013 (scenes 12 and 13), colour-coded by scene. North is to the left.

4.6 South Georgia

For South Georgia we have improved the former glacier outlines from 2003 with a Landsat ETM+ scene from 2002 (path-row 206-98) that had less seasonal snow in the northern slope of the island but clouds along the southern slope. New glacier outlines have been created from a cloud-free Landsat 8 OLI scene acquired in 2016. Also this scene has been snow-corrected in the north with a scene acquired in the year before (but is also cloud covered in the south). Table 4.5 is listing the details of the four scenes, Fig. 4.5 shows the derived 2016 outlines.

Nr.	Date	Day	Comment	Nr.	Date	Day	Comment
1	2002 01 03	3	clouds in the south	3	2015 02 16	65	clouds in the south
2	2003 02 07	38	some seasonal snow	4	2016 02 19	50	some seasonal snow

Table 4.5: Landsat scenes used for the former and the new inventory of South Georgia.

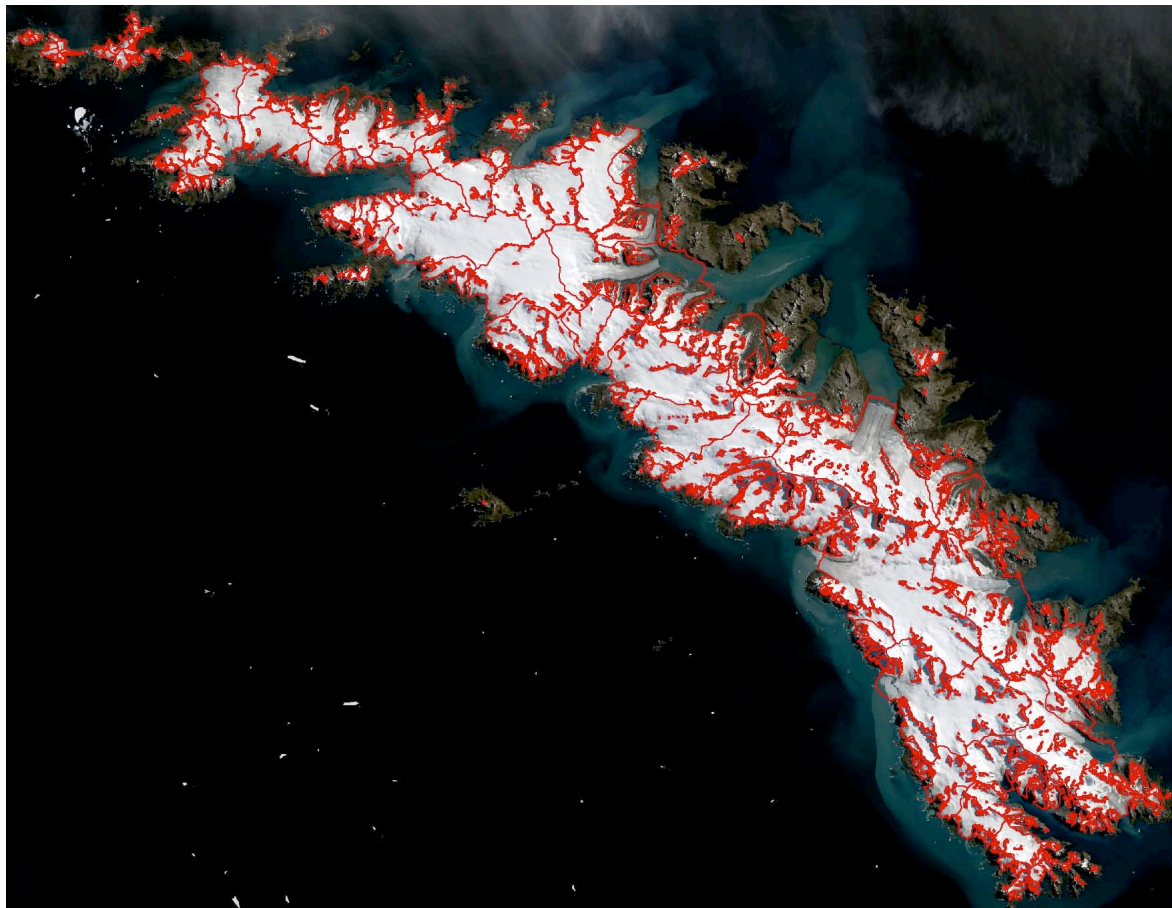


Fig. 4.5: Glacier outlines for South Georgia from 2003 shown on scene 4 in the background.

5. Elevation Change (ALT)

Elevation change products were generated for the Greenland peripheral glaciers and ice caps using data from the CryoSat-2 SIRAL instrument. The dataset covers RGI region 5.

5.1 Greenland (peripheral glaciers)

Elevation change rates are calculated within 9091 2km x 2km grid cells (polar stereographic projection) that fall within the RGI Greenland Periphery mask. The 1345406 input datapoints used in the calculations are from the period July 2010 to December 2014. A plane fit method was used, based on data from the L2I LRM and SARIn products.

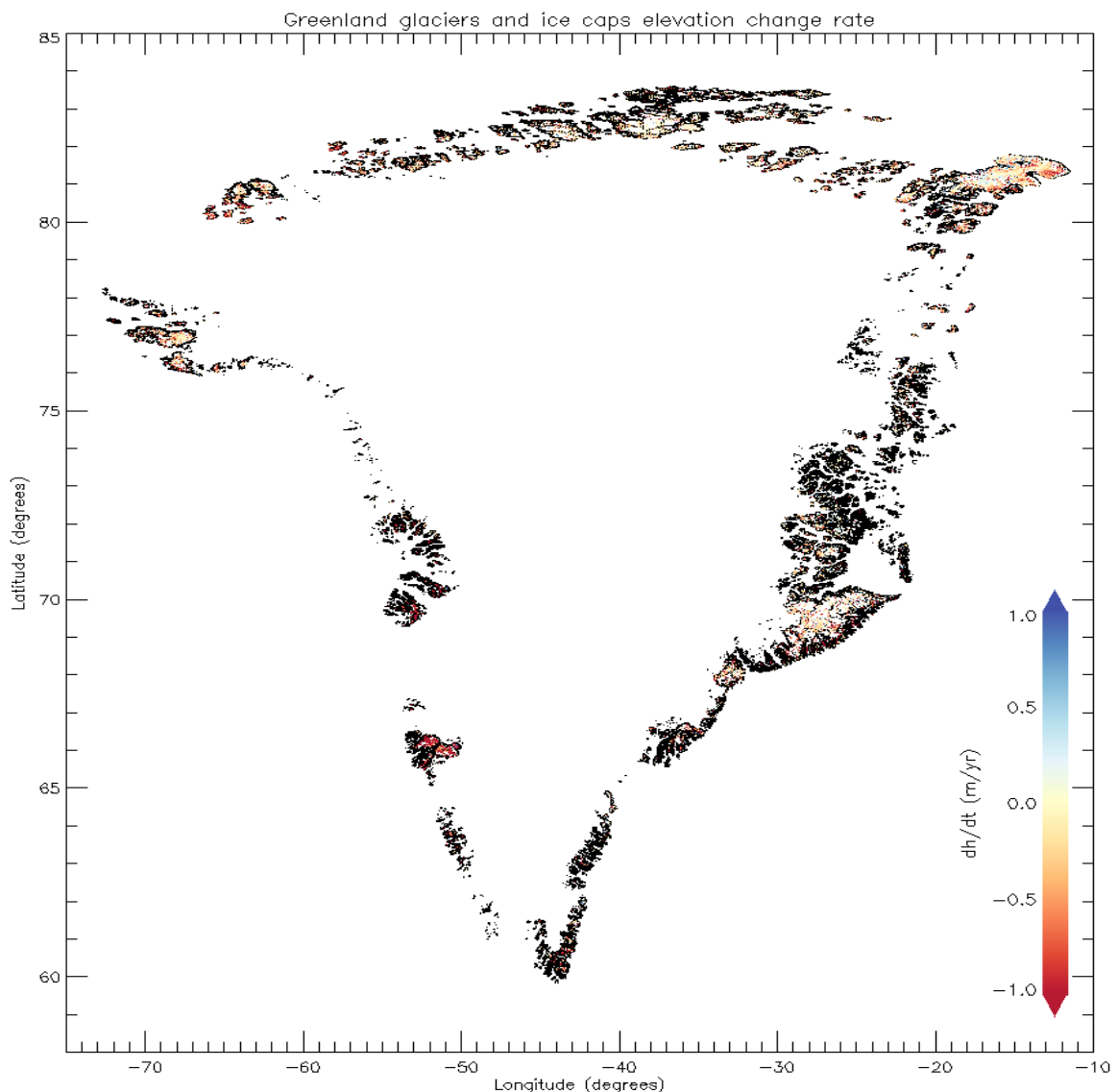
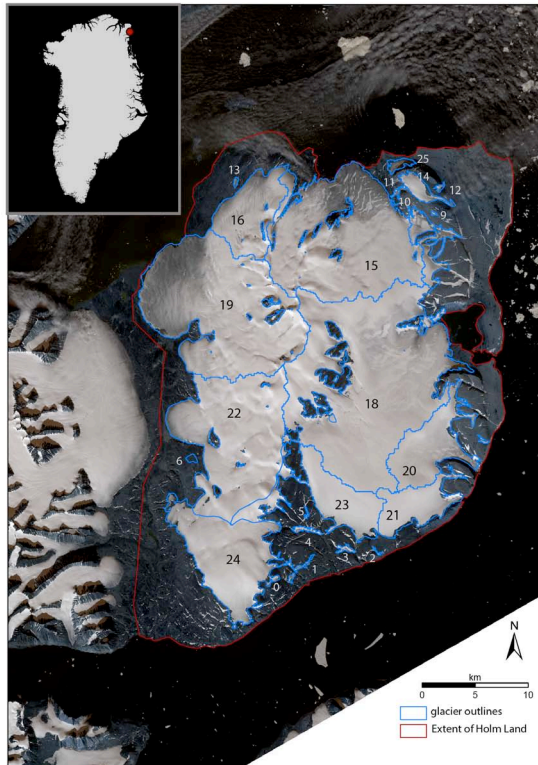


Figure 5.1: Elevation change rates from CryoSat-2 data, 2010-2014, in the Greenland Periphery.

6. Elevation Change (DEM)

6.1 Greenland



For the Holm Land Peninsula in north-eastern Greenland (see Fig. 6.1) we have calculated elevation changes between the ArcticDEM from around 2013 and the AeroDEM from 1978. Both DEMs were resampled to the common resolution of 25 m and co-registered. The Arctic DEM has some data voids and the Aero DEM local interpolation artefacts. These were considered differently to derive the elevation changes shown in Fig. 6.2.

Fig. 6.1: The new glacier inventory for central western Greenland (yellow outlines) are shown on top of the three satellite images used to create the inventory).

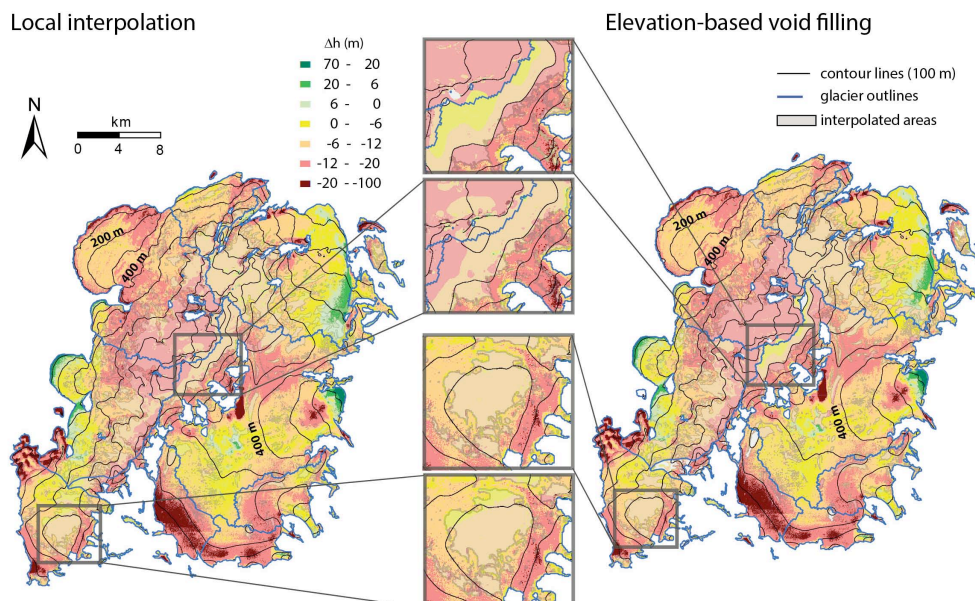


Fig. 6.2: Elevation changes obtained for the ice cap on Holm Land peninsula (Greenland) by subtracting the ArcticDEM (from 2012-2015) from the AeroDEM (from 1978) using two different methods of interpolation.

6.2 Svalbard

Elevation changes are derived for two epochs, 1936-1990 and 1990-2008, for a large region containing southern Spitsbergen. In the first epoch, the oldest topographic maps are compared to a national DEM (20 m resolution) derived from vertical aerial images acquired in 1990. The accuracy of the oldest maps are limited, however, with the 54-year time epoch, individual changes larger than 0.2 m per year are significant. For the newer epoch, the 1990 DEM is compared with a satellite optical DEM (40 m resolution) from SPOT5 acquired during the IPY-SPIRIT mission (Korona et. al. 2009). Although the original DEM data is more accurate, the time period between DEMs is smaller. Therefore, individual changes greater than 0.4 m per year are considered significant.

In southern Spitsbergen, the comparison between elevation changes derived in the two epochs show that glacier thinning on the tongues has increased (Fig. 6.3). In both epochs, regions of positive changes occur. Modest increases often occur in relation to surge-type glaciers in which the glaciers tend to build up in the accumulation areas. During the second epoch, a number of surging glaciers are apparent as large thickness increases are measured on some tongues.

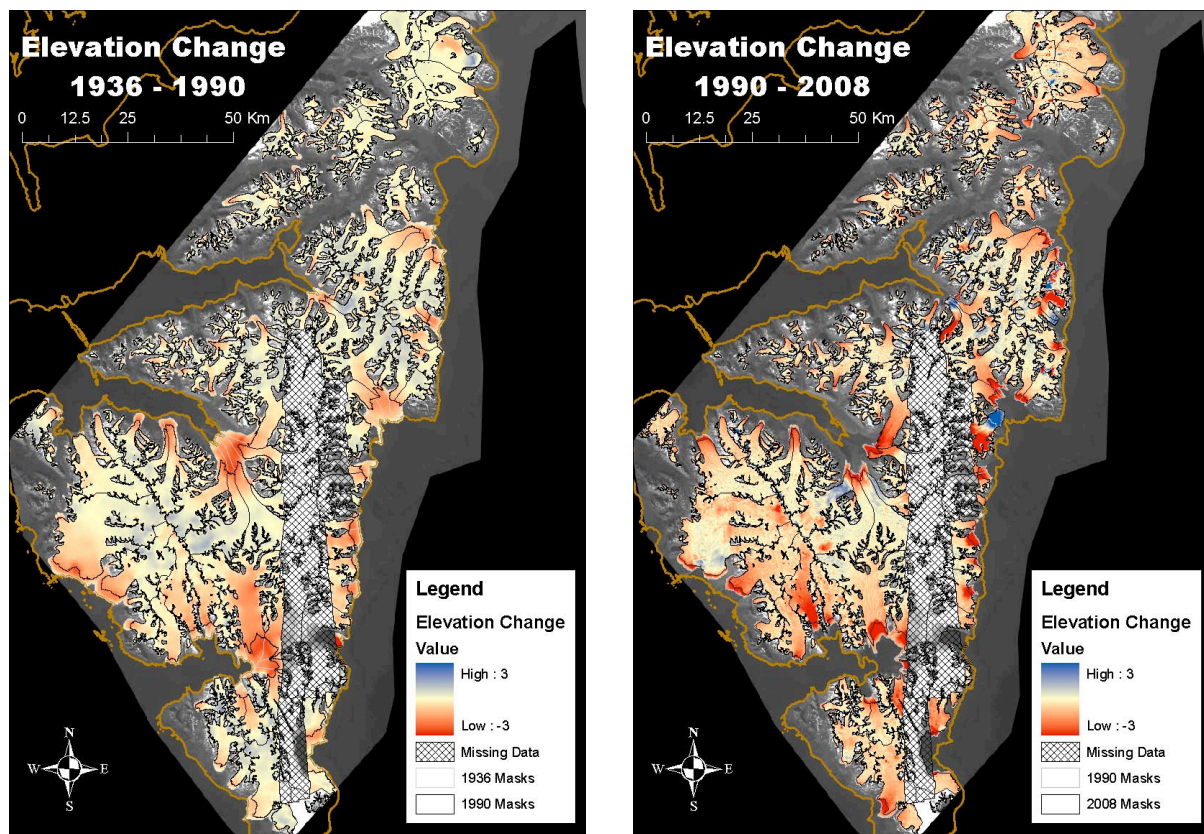


Figure 6.3: Elevation changes from two epochs spanning the past 80 years. The first epoch (left) compares the oldest national topographic maps from Svalbard in 1936 to a DEM derived from vertical aerial photographs in 1990. Right: The second epoch (1990-2008) compares the DEM to a satellite DEM derived from SPOT5 during the IPY-Spirit mission (Korona et al. 2009).

TanDEM-X products are tested in Svalbard to assess the feasibility and accuracy of these DEMs for glacier elevation change estimates. We tested the TanDEM-X Intermediate DEM (IDEM) product against the national DEM. The IDEM is a merged compilation of individually processed TanDEM-X strip acquisitions over a period of two or more years. The related merging of individual DEM tiles is apparent across the archipelago, with horizontal coregistration vectors that vary depending on region. Figure 6.4 shows an example of artifacts from the merging process in which a distinct linear feature running east to west is apparent as a result of varying horizontal co-registration parameters within the IDEM product. In this case, the co-registration parameters are solved for the southern section, while the northern section still contains aspect-dependent biases from failed co-registration. Nonetheless, the precision of the IDEM compared to the DEM derived from aerial photography is about 2-3 m as revealed by the standard deviation on terrain assumed to be stable (inset Fig. 6.4).

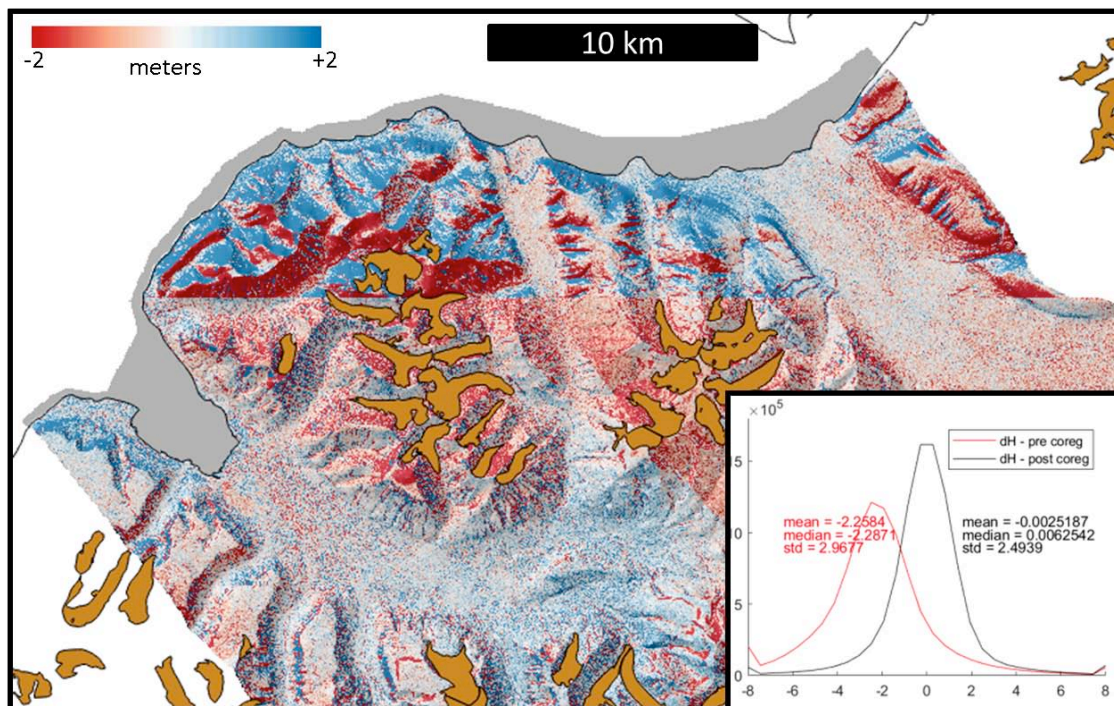


Figure 6.4: Stable terrain elevation differences between the TanDEM-X IDEM product and a national DEM derived from vertical aerial photographs. A distinct linear feature running east-west shows a merging artefact between two adjacent IDEM tiles. The inset shows the histograms of stable terrain differences before and after uniform co-registration between the DEMs.

6.3 Caucasus

Elevation changes are derived between 97 ASTER scenes acquired 2014-2017 and the SRTM C-Band product for the Caucasus Mountains. The ASTER scenes are produced using the MMASTER workflow described by [Girod et al. \(2017\)](#), using the SRTM as a secondary DEM to remove jitter-induced errors. The DEMs are co-registered to the SRTM, with an average RMS difference over low-slope, stable terrain of 13.9 m. The dDEM s are re-sampled to 100 m resolution, then averaged to create a composite map of elevation change rates. Some clear

artefacts are present in the final product of elevation change rates, particularly near the summit of Mt. Elbrus (Fig. 6.5), though the map as a whole shows a clear thinning signal at the lower elevations of most glaciers. Recent studies (e.g. [Berthier et al. 2018](#)) have suggested that the SRTM C-band should be avoided for estimates of glacier volume change, especially in the Northern Hemisphere and especially over timescales of less than 20 years. This recommendation is due to penetration depths that may be much larger than previously assumed. Thus, these data should not be used for quantitative estimates of volume change in the Caucasus, and we provide only a first qualitative assessment of elevation changes here.

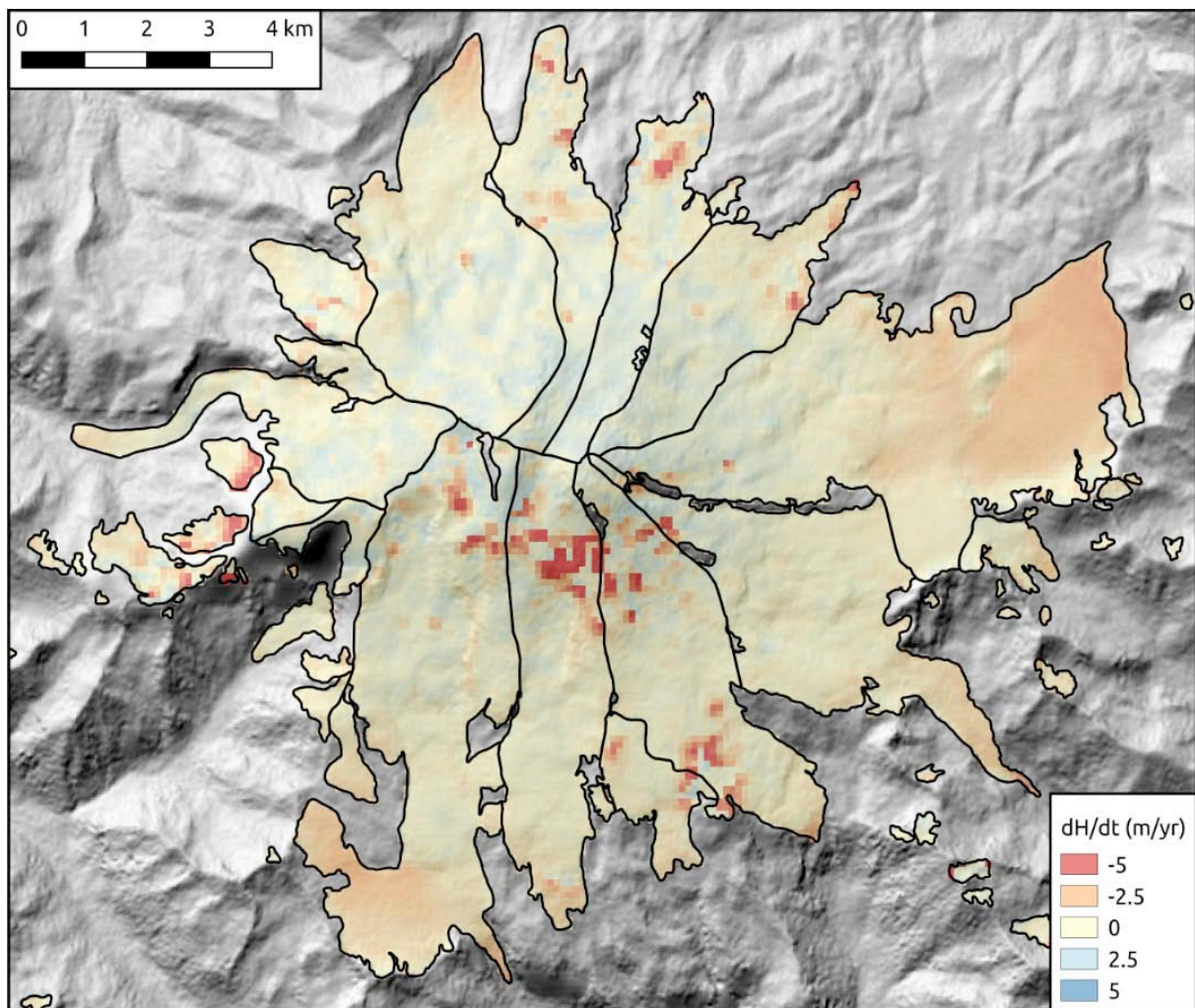


Figure 6.5: Elevation changes over Mt. Elbrus (Caucasus) as derived from ASTER scenes acquired over the 2014 to 2017 period and the SRTM C band DEM.

7. Velocity

Table 7.1 provides an overview on the satellite SAR scenes used to generate the datasets described in Sections 7.1, 7.2, 7.5 and 7.6. The scenes used to create the circum Arctic mosaic presented in Section 7.3 had been listed in the year two update of this document and are not repeated here. However, an in-depth analysis has been performed in the meantime (Strozzi et al. 2017) and key results are presented in section 7.3. Also Section 7.4 is presenting the key results of a detailed analysis, here related to the surge of Hispar Glacier in 2015/16 (Paul et al. 2017). The SAR and optical scenes used for this analysis are listed in section 7.4. In general all SAR scenes were geocoded with the SRTM v4 DEM (void-filled version).

RGI	Region	Sensor	Date range	ΔT (days)	Remarks	Section
5	Greenland	S1	2014-2017	6d-1yr	Annual Mosaic & timeseries	7.1
7	Svalbard	S1	2015-2017	6d-2yr	Mosaic & timeseries	7.2
3,4,7,9	Circum Arctic	several	2 periods	var.	Mosaic for 2 time periods	7.3
14	Karakoram	S1, L7/8	2015-2016	var.	Time series Hispar Glacier	7.4
17	Patagonia	S1	2014-2017	3 yr	Averaged over entire period, multiple tracks merged	7.5
19	South Georgia	S1	2016	3 yr	Averaged over entire period, multiple tracks merged	7.6
19	Alexander Island	PALSAR	2010	5 m	Averaged over entire period, multiple tracks merged	7.7

Table 7.1: The microwave datasets used for velocity product generation in year 2 of phase 2. Abbreviations: TSX: TerraSAR-X, GIC: glaciers and ice caps, FBD: Fine Beam Double polarisation, FBS: Fine Beam Single polarization.

7.1 Greenland

Three ice sheet wide velocity products for Greenland including the peripheral glaciers, are produced from Sentinel-1 data (Table 7.2 and Fig. 7.1) as a combined product for the Greenland and Glaciers CCI projects. The ice velocity maps are derived using iterative offset tracking, permitting to acquire the full range of velocities in a single swath while keeping the matching window at a minimum. The latest map (2016/17) includes data from both Sentinel-1A and 1B data and is acquired within a period of approximately 2 months during the latest winter campaign. The product also includes a valid pixel count map and an uncertainty map (Fig. 7.2). Aside from the annual winter mapping campaigns, Sentinel-1 provides continuous coverage in IW mode for the entire Greenland Ice Sheet margin since October 2014, with 6 to 12-day repeat pass periods. This data is used to produce a long and dense time series of ice velocity for major outlets and peripheral glaciers. The data sets are available at 200 m grid spacing along with some basic tools for time series analysis through the ENVEO Cryoportals (<http://cryoportals.enveo.at/>).

Table 7.2: Sentinel-1 annual ice sheet wide velocity maps.

Sensor	Period
Sentinel-1A	1.11.2014 - 1.12.2015
Sentinel-1A	23.12.2015 - 31.3.2016
Sentinel-1A & 1B	23.12.2016 - 27.2.2017

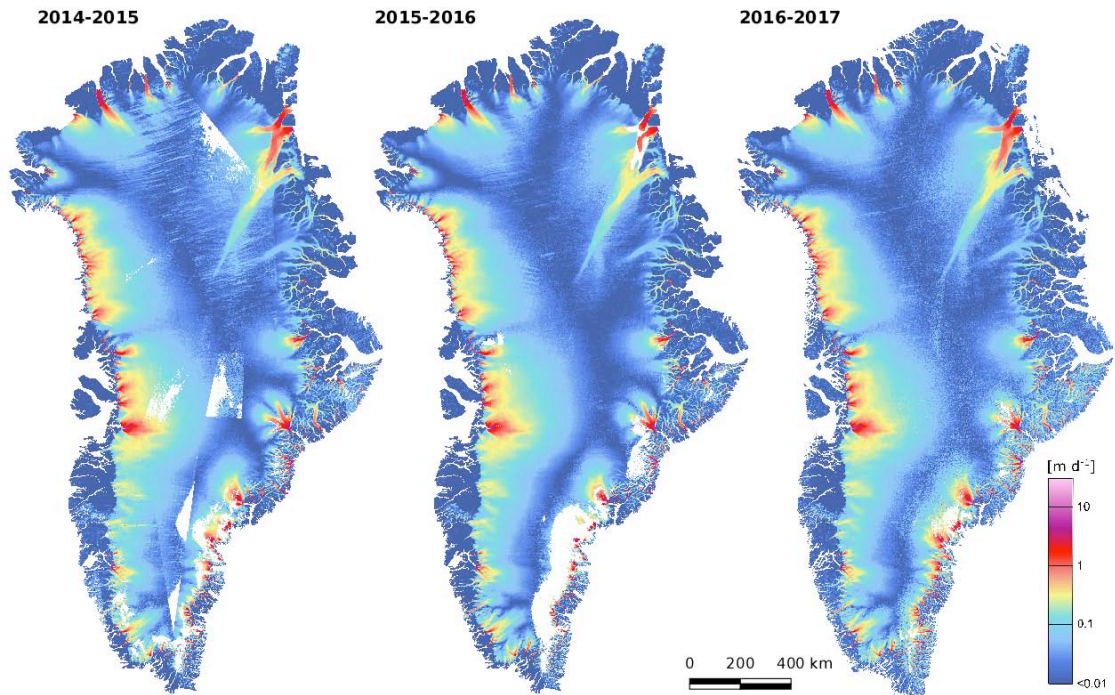


Figure 7.1: Sentinel-1 annual ice sheet wide ice velocity map, 2014/15, 2015/16 and 2016/17.

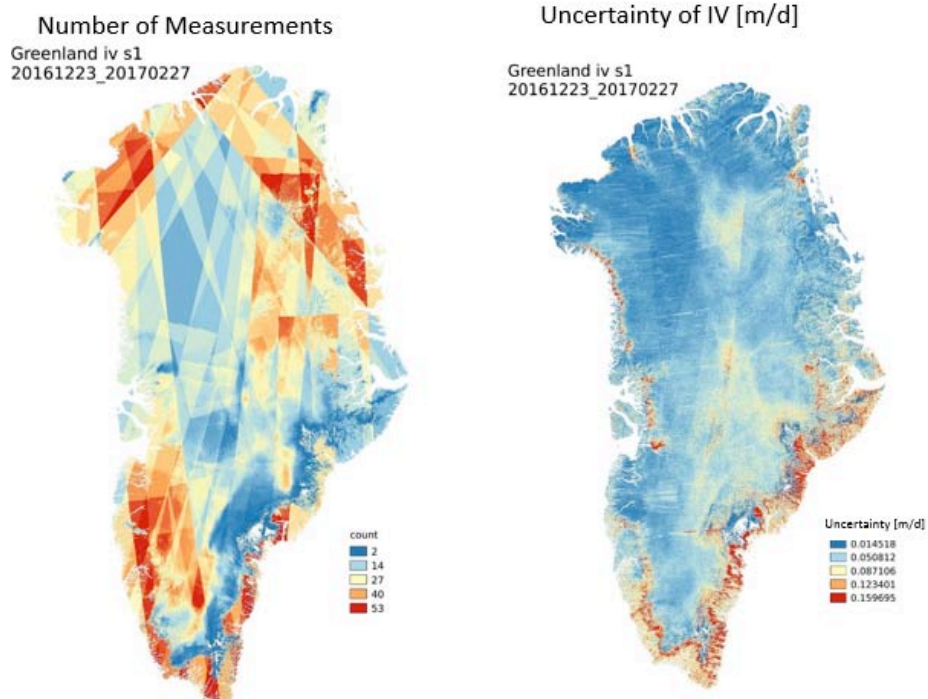


Figure 7.2: Pixel count and uncertainty map provided with the ice sheet IV map for 2016/17.

7.2 Svalbard

A complete ice velocity mosaic covering all major glaciers and ice caps of the Svalbard Archipelago is produced using Sentinel-1 data (Fig. 7.3). The ice velocity is derived by SAR offset tracking using Sentinel-1 image pairs acquired in Interferometric Wide Swath (IW) mode and averaged over the period Jan 2015 to Jan 2017. The velocity map is gridded to 250 m and clipped using an ocean mask that is based on Landsat imagery with calving fronts updated to 2014-2016. The Norwegian Polar Institute Terrenmodell Svalbard (20 m) is used for topographic reference and RGI 5.0 glacier outlines are used for validation. Time series of ice velocity are available for major outlet glaciers and accessible through the ENVEO Cryoport (<http://cryoport.enveo.at/>) (Fig. 7.4).

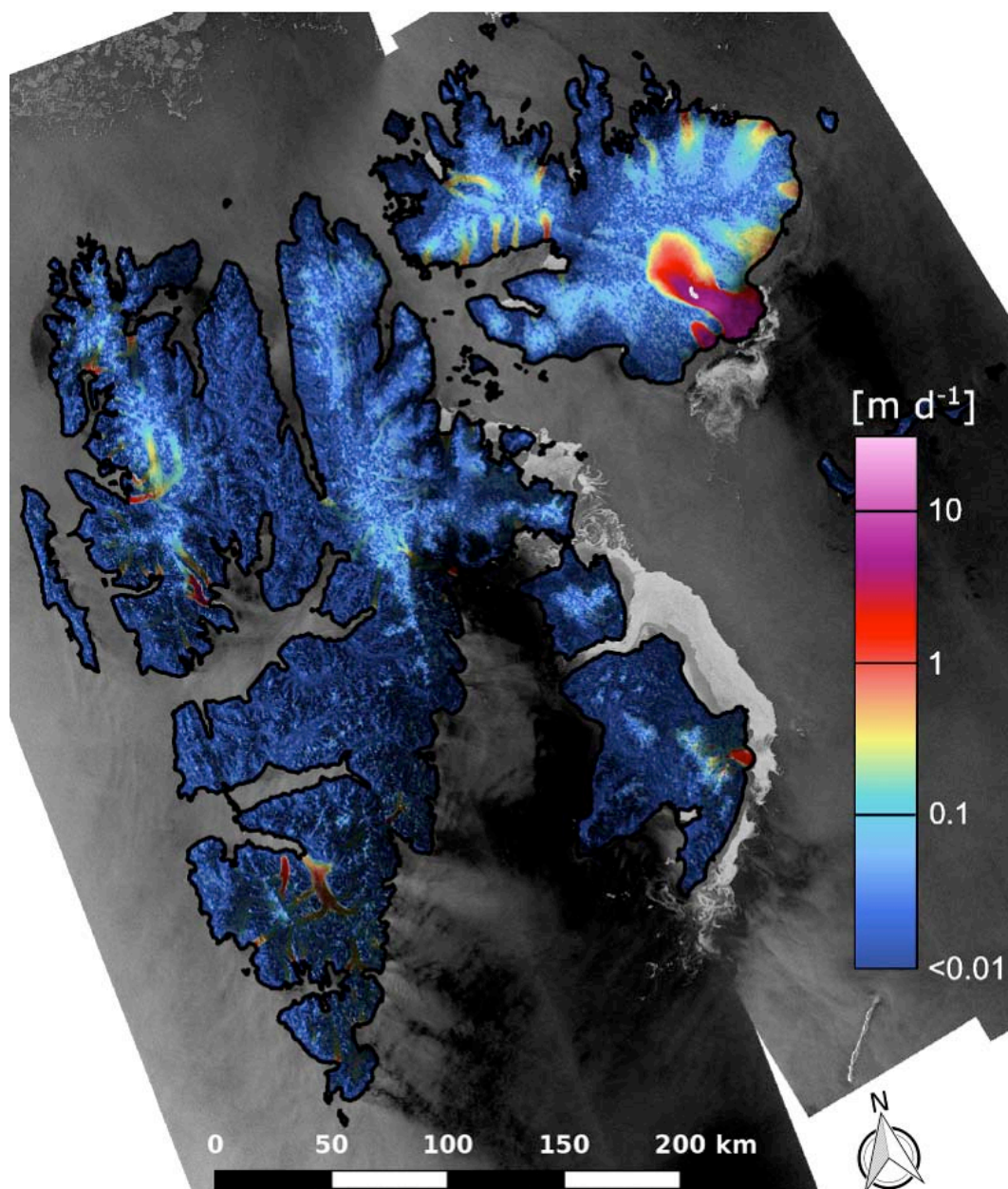


Figure 7.3: Ice velocity map of Svalbard from Sentinel-1 data acquired from Jan 2015 to Jan 2017. Background: Sentinel-1 amplitude mosaic.

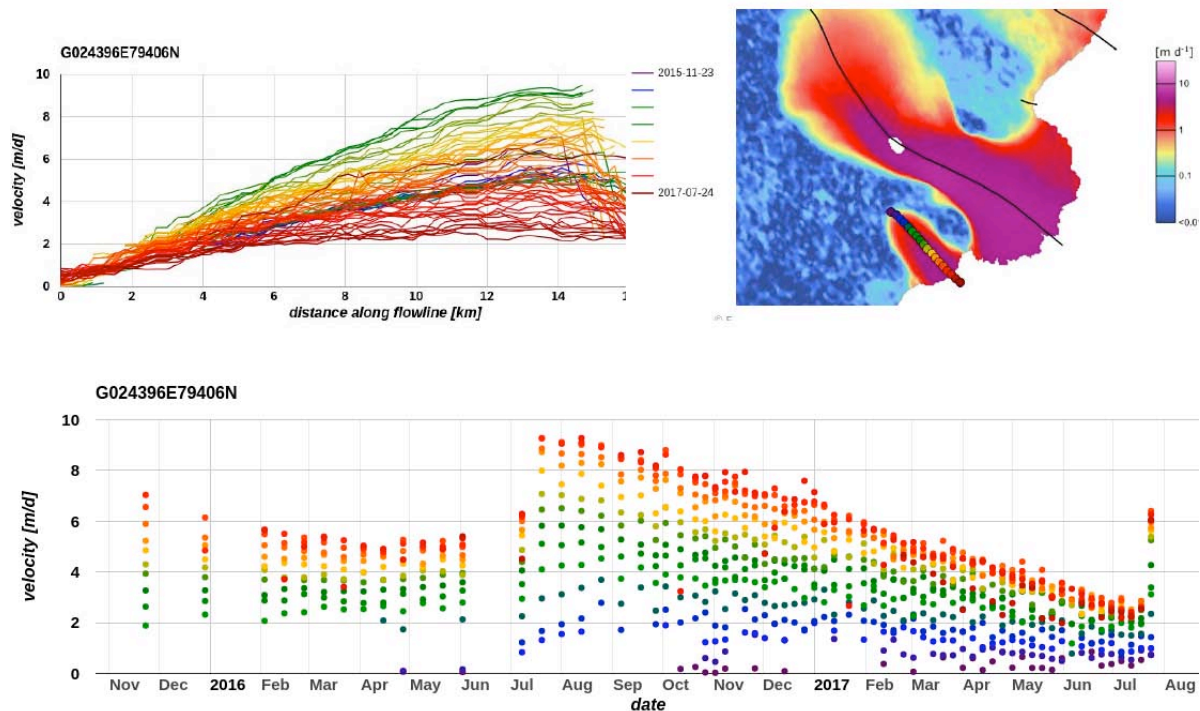


Figure 7.4: Time series of ice velocity along the centre line profile of a surging outlet glacier on southern Austfonna Ice Cap.

7.3 Circum-Arctic glaciers

We computed circum-Arctic surface velocity maps of glaciers and ice caps over the Canadian Arctic, Svalbard and the Russian Arctic for at least two times between the 1990s and 2017 using satellite SAR data (Strozzi et al. 2017). Our analyses were mainly performed with off-set-tracking of ALOS-1 PALSAR-1 (2007–2011) and Sentinel-1 (2015–2017) data. In certain cases JERS-1 SAR (1994–1998), TerraSAR-X (2008–2012), Radarsat-2 (2009–2016) and ALOS-2 PALSAR-2 (2015–2016) data were used to fill-in spatial or temporal gaps.

In general, we observed that changes in the flow of glaciers and ice caps between the 1990s and 2017 over the Canadian Arctic are minor compared to those observed over Svalbard and the Russian Arctic. While a gradual slow-down dominates over many glaciers in the Canadian High Arctic, a steady increase of frontal velocities along with a retreat of frontal positions is common for many glaciers over the Svalbard archipelago and the Russian Arctic. Several of them are surging with much higher flow velocities than usual.

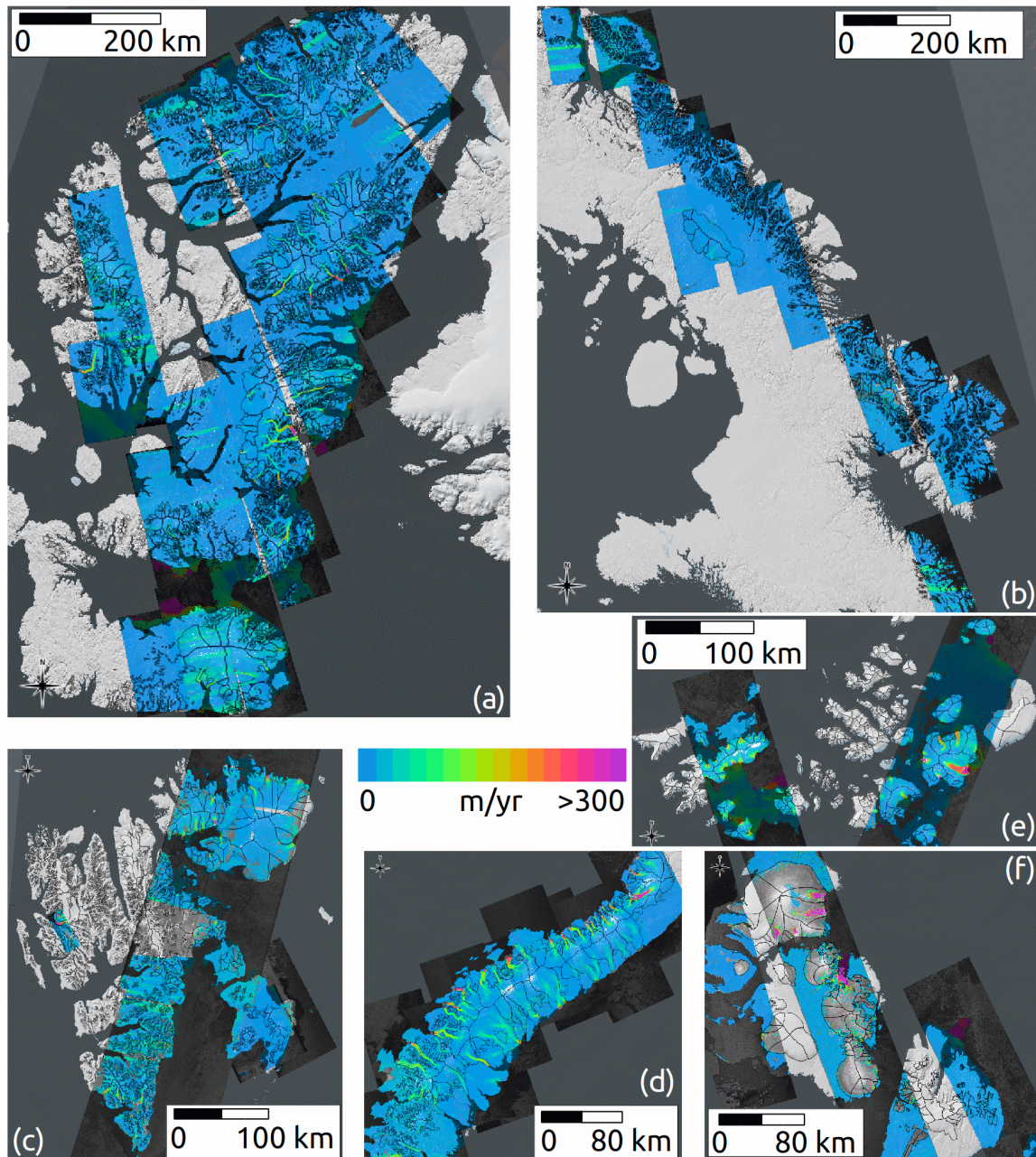


Figure 7.5: Ice velocity maps for (a) the Canadian Arctic North from ALOS-1 PALSAR-1 data of 2007 to 2011; (b) the Canadian Arctic South from ALOS-1 PALSAR-1 data of 2007 to 2011; (c) the Svalbard Archipelago from JERS-1 SAR data of 1994 to 1998 complemented by ALOS-1 PALSAR-1 data of 2010–2011 to the east and TerraSAR-X data of 2008 to the west; (d) Novaya Zemlya from ALOS-1 PALSAR-1 data of 2008 to 2009; (e) Franz-Josef Land from JERS-1 SAR data of 1998 in the east and ALOS-1 PALSAR-2 data of 2010 in the west; and (f) Severnaya Zemlya from ALOS-1 PALSAR-1 data of 2010.

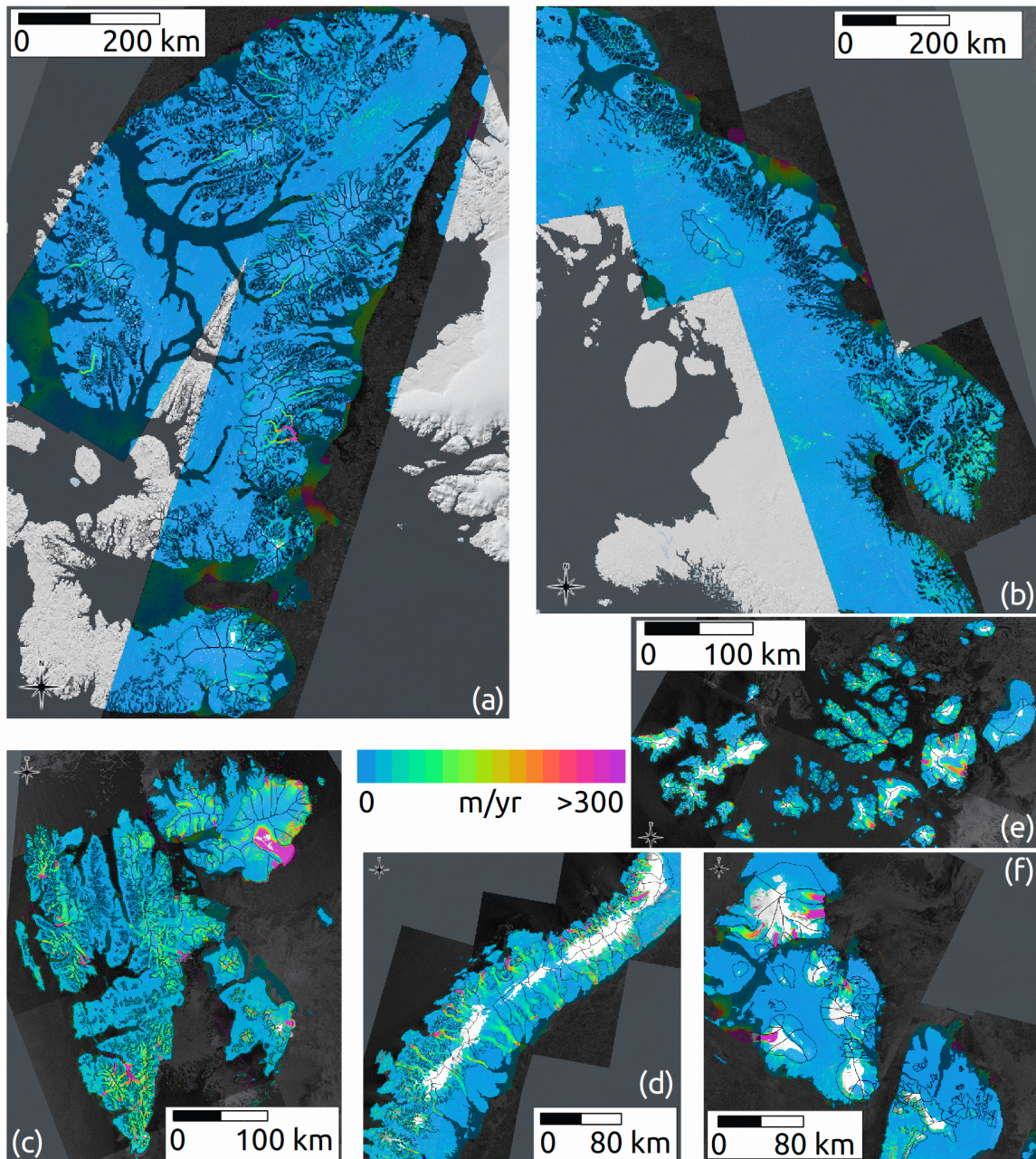


Figure 7.6: Ice velocity maps from Sentinel-1 SAR winter data of (a) 2015 over the Canadian Arctic North; (b) 2016 over the Canadian Arctic South; (c) 2015–2016 (average) over the Svalbard Archipelago; (d) 2017 over Novaya Zemlya; (e) 2016 over Franz-Josef Land; and (f) 2016–2017 over Severnaya Zemlya.

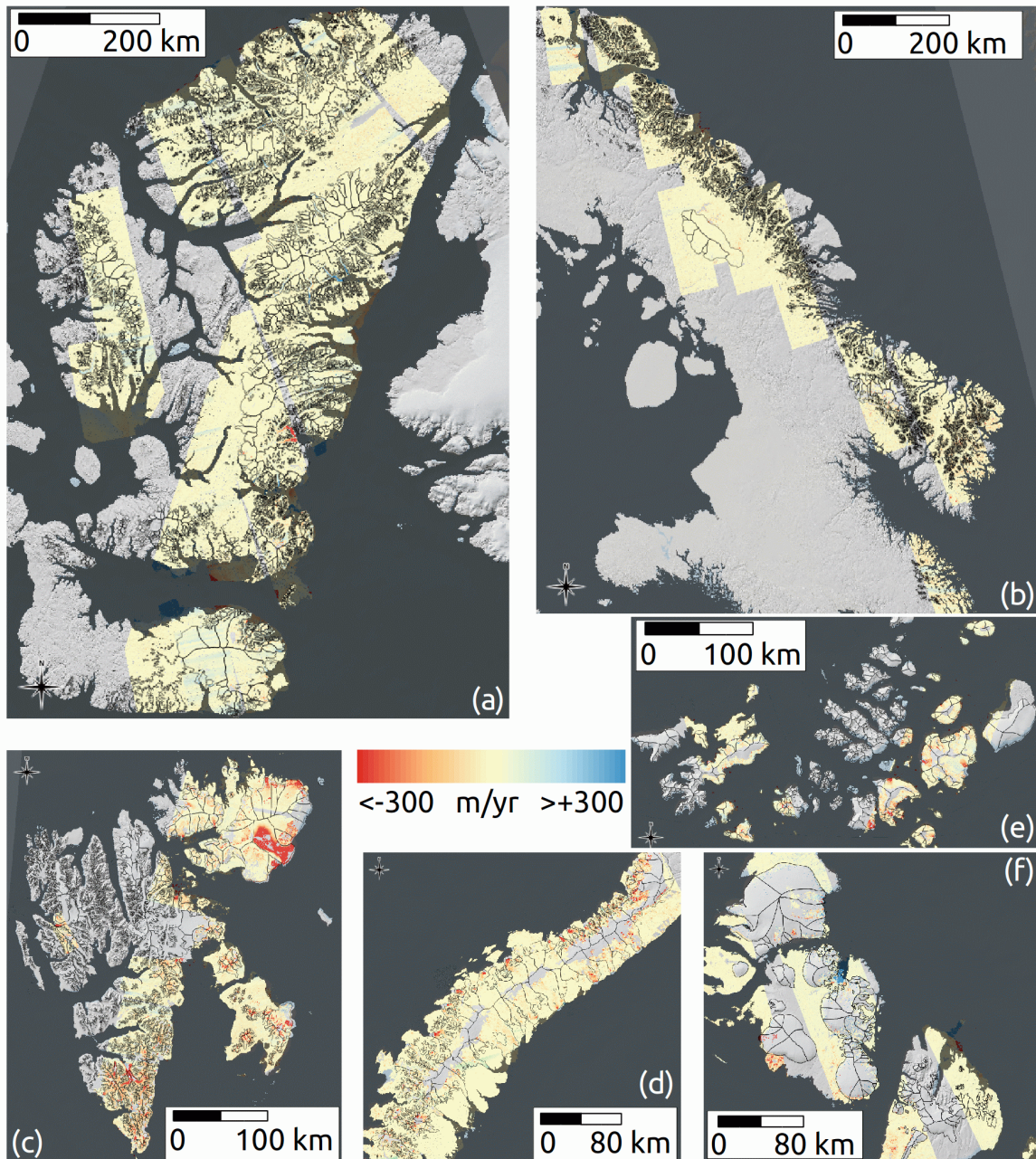


Figure 7.7: Difference map of the ice velocity results of Figure 7.5 (1994–2011) and 7.6 (2015–2017) over (a) the Canadian Arctic North, (b) the Canadian Arctic South, (c) the Svalbard Archipelago, (d) Novaya Zemlya, (e) Franz-Josef Land and (f) Severnaya Zemlya.

The latter developments can be well traced based on the very high temporal sampling of Sentinel-1 acquisitions since 2015, revealing new insights in glacier dynamics. For example, surges on Spitsbergen (e.g., Negribreen, Figure 7.8) have a different characteristic and timing than those over Eastern Austfonna and Edgeoya (e.g., Stonebreen, Figure 7.9). Events similar to those ongoing on Eastern Austfonna were also observed over the Vavilov Ice Cap on Severnaya Zemlya and possibly Simony Glacier on Franz-Josef Land.

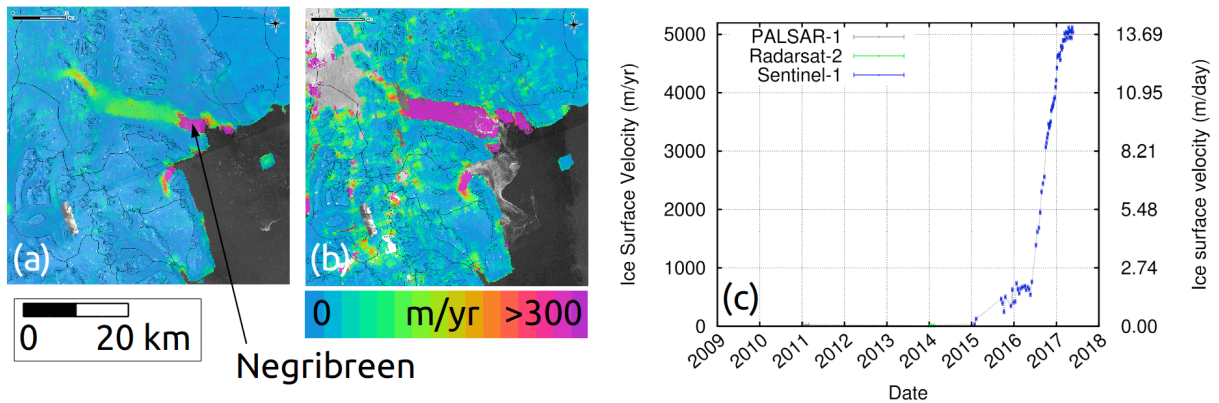


Figure 7.8: Ice surface velocity maps for Negribreen on Spitsbergen (Svalbard) from Sentinel-1 data of the time periods 01/10/2015 to 13/10/2015 (a) and 31/10/2016 to 12/11/2016 (b) and time-series of velocity close to the front from 2011 to 2017 (c). The arrow points to the location used for the time series.

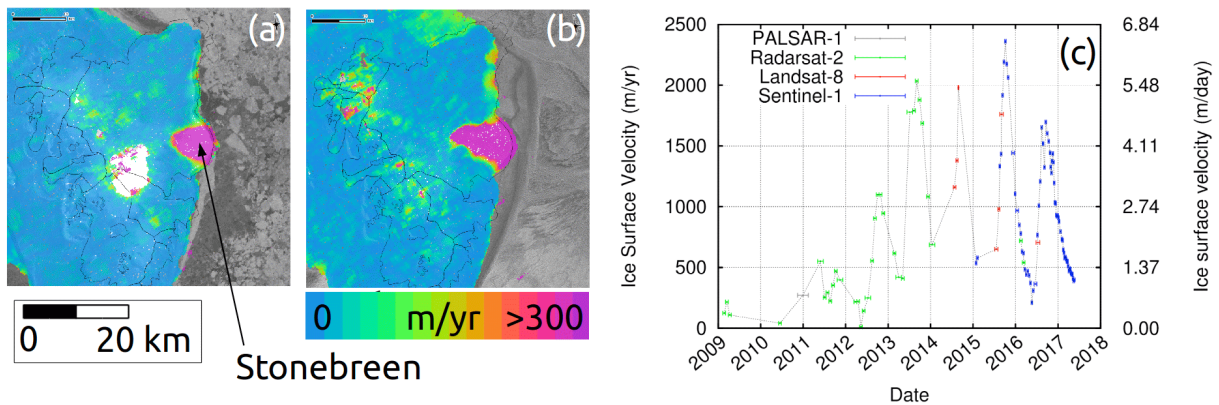


Figure 7.9: Ice surface velocity maps for Stonebreen on Edgeøya (Svalbard) from Sentinel-1 data of the time periods 21/01/2015 to 02/02/2015 (a) and 27/02/2017 to 11/03/2017 (b) and time-series of velocity close to the front from 2009 to 2017 (c).

Collectively, there seems to be a recently increasing number of glaciers with frontal destabilization over Eastern Svalbard and the Russian Arctic compared to the 1990s. The fact that, largely unexpected, destabilizations of a few glaciers are able to dominate the total calving flux and thus sea-level impact from Arctic glaciers and ice caps, at least over time-scales of years to decades, underlines how important it is to have a reliable, accurate and automatic, all-weather and year-round satellite-based glacier velocity monitoring system available.

7.4 Karakoram

For the Hispar Glacier in the Karakoram we have created time series of surface flow velocities from Landsat 7 and 8, Sentinel 1 and Radarsat 2 to document and analyse its 2015/16 surge and its flow fields in the years before (Paul et al. 2017). Tables 7.3 and 7.4 are listing the satellite scenes used to create the flow fields, whereas Figures 7.10 and 7.11 show selected results of that study in a time versus distance plot (calculated along the central flowline) and the pre-surge velocity variability for the entire glacier in individual panels, respectively.

Date 1	Date 2	Δt	Sensor	Date 1	Date 2	Δt	Sensor
5 July 2013	21 July 2013	16	L8 OLI	29 Jan 2014	3 April 2014	64	L8 OLI
21 July 2013	7 Sep 2013	48	L8 OLI	3 April 2014	6 June 2014	64	L8 OLI
7 Sep 2013	9 Oct 2013	32	L8 OLI	6 June 2014	8 July 2014	32	L8 OLI
9 Oct 2013	25 Oct 2013	16	L8 OLI	8 July 2014	24 July 2014	16	L8 OLI
25 Oct 2013	10 Nov 2013	16	L8 OLI	24 July 2014	25 Aug 2014	32	L8 OLI
10 Nov 2013	26 Nov 2013	16	L8 OLI	25 Aug 2014	05 Nov 2014	16	L8 OLI
26 Nov 2013	12 Dec 2013	16	L8 OLI	5 Nov 2014	8 Jan 2015	64	L7 ETM+
12 Dec 2013	29 Jan 2014	48	L8 OLI	8 Jan 2015	9 Feb 2015	32	L7 ETM+

Table 7.3: Satellite scenes used to calculate flow velocities from the time before the surge.

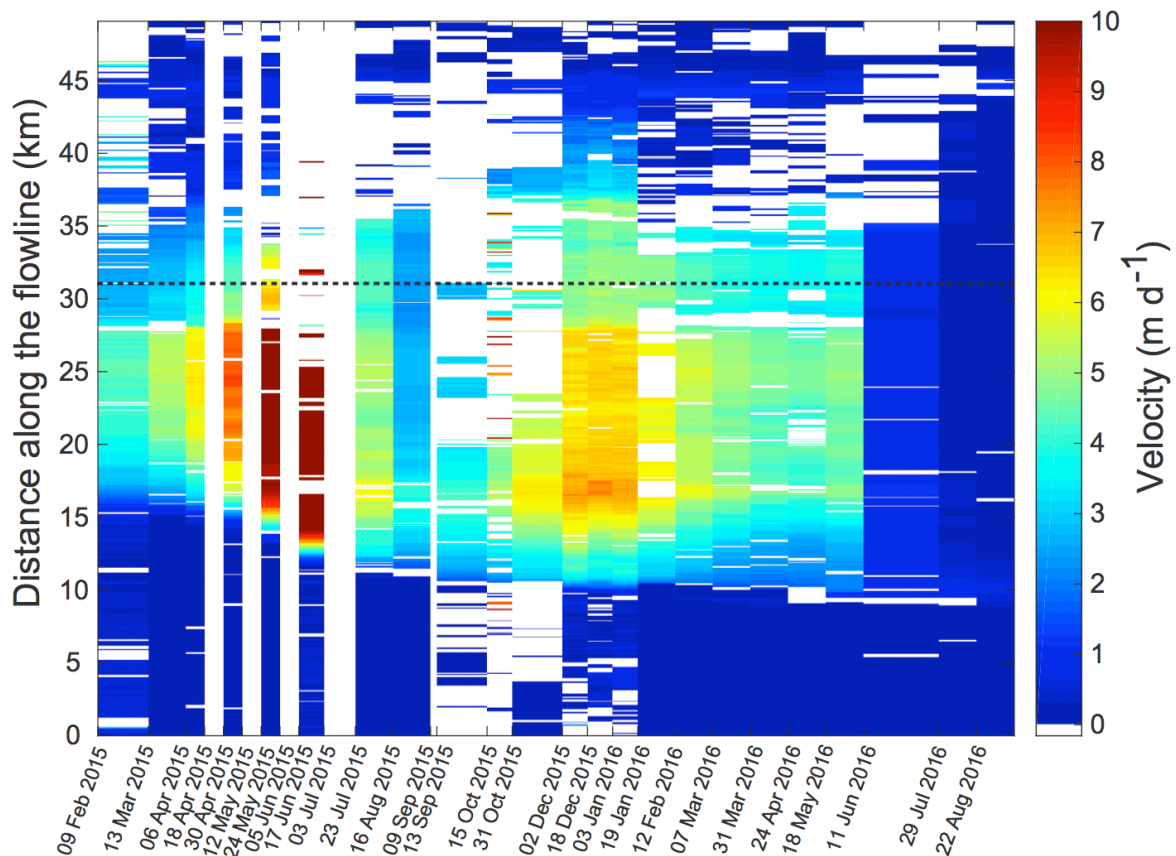


Fig. 7.10: Time versus distance plot of flow velocities for the main surge with its two peaks. Maximum values reached 14 m per day in May 2015.

Date 1	Date 2	Δt	Sensor	Date 1	Date 2	Δt	Sensor
13 March 15	6 April 15	24	Sentinel-1	18 Dec 15	3 Jan16	16	L8 OLI
6 April 15	18 April 15	12	Sentinel-1	3 Jan 16	19 Jan 16	16	L8 OLI
30 April 15	12 May 15	12	Sentinel-1	19 Jan 16	12 Feb 16	24	Sentinel-1
24 May 15	5 June 15	12	Sentinel-1	12 Feb 16	7 March 16	24	Sentinel-1
17 June 15	3 July 15	16	L7 ETM+	07 March 16	31 March 16	24	Sentinel-1
23 July 15	16 Aug15	24	Sentinel-1	31 March.16	24 April 16	24	Sentinel-1
16 Aug 15	9 Sep 15	24	Sentinel-1	24 April 16	18 May 16	24	Sentinel-1
13 Sep 15	15 Oct15	32	L8 OLI	18 May 16	11 June 16	24	Sentinel-1
15 Oct 15	31 Oct15	16	L8 OLI	11 June 16	29 July 16	48	Sentinel-1
31 Oct 15	2 Dec 15	32	L8 OLI	29 July 16	22 Aug 16	24	Sentinel-1
2 Dec15	18 Dec 15	16	L8 OLI	22 Aug 16	15 Sep16	24	Sentinel-1

Table 7.4: Satellite scenes used to calculate flow velocities for the main surge.

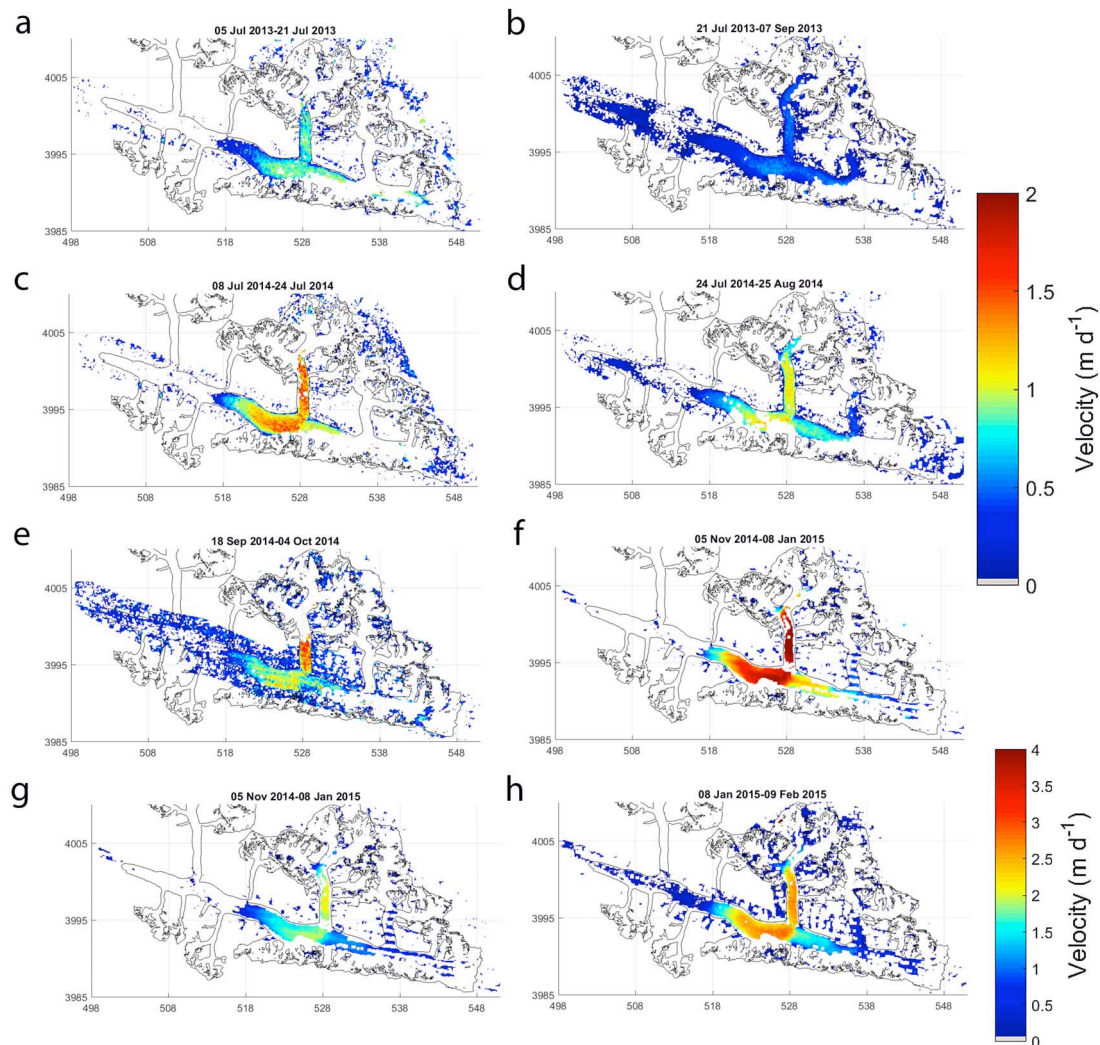


Fig. 7.11: Flow acceleration of Hispar Glacier during summer 2013/14 before the surge (a to d) and initiation of the main surge by a tributary (e). Panels f and g are from the same period but using a different colour scale to reveal the flow acceleration in winter 2015 (h).

7.5 Patagonia

For the Southern Patagonian Ice Field (SPI) a complete coverage of ice surface velocity is available derived from Sentinel-1 data (Fig. 7.12). The velocity map is compiled applying feature tracking using Sentinel-1 repeat image pairs acquired in IW mode and averaged over the period 2014 to 2017. The data set is posted at 200 m and provided in WGS 84 / UTM zone 18S projection. For geocoding of the product we use the TanDEM Global DEM for Patagonia with gaps filled with SRTMv4. Updated glacier outlines, derived from Landsat images acquired in February 2017, were used for clipping to glacier areas and for validation of the product. More detailed information on the produced datasets can be found in the metadata information sheet provided with each product in the CRDP database.

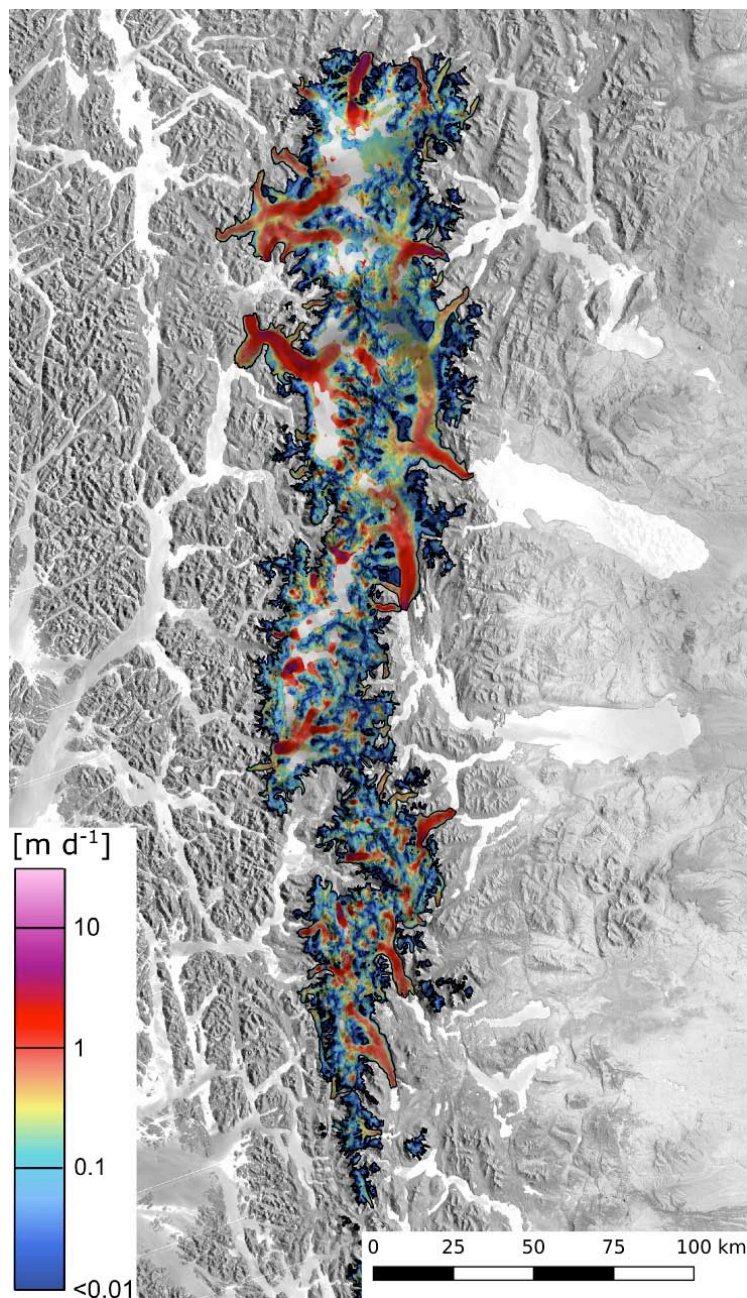


Figure 7.12: Mosaic obtained from Sentinel 1 data from 2014-2017 for the Southern Patagonian Icefield. Background: S1 amplitude image (July/Aug 2016).

7.6 South Georgia

The velocity products for South Georgia have been extended with a data set derived from Sentinel-1 data acquired in 2016 (Fig 7.13). The velocity field provides excellent coverage for the entire island, in total covering more than 90% of the glaciers. Velocities are derived by applying feature tracking using Sentinel-1 image pairs acquired in IW mode and averaged over the period July 2016 to October 2016. The data set is posted at 200 m and provided in WGS 84 / UTM zone 24S projection. The ASTER Global DEM V002 is used for topographic reference and to create an ocean/land mask. RGI 5.0 glacier outlines were used for validation of the product (mask for stable terrain off glaciers).

The Glaciers_cci IV products covering South Georgia now provide three snapshots in time: 2010 (ALOS PALSAR), 2013 (TerraSAR-X) and 2016 (Sentinel-1). All products are derived from data acquired within a timeframe of 2-4 months and roughly overlap in terms of seasonal coverage (winter season), providing a good means for intercomparison. More detailed information on the produced datasets can be found in the metadata information sheet provided with each product in the CRDP database.

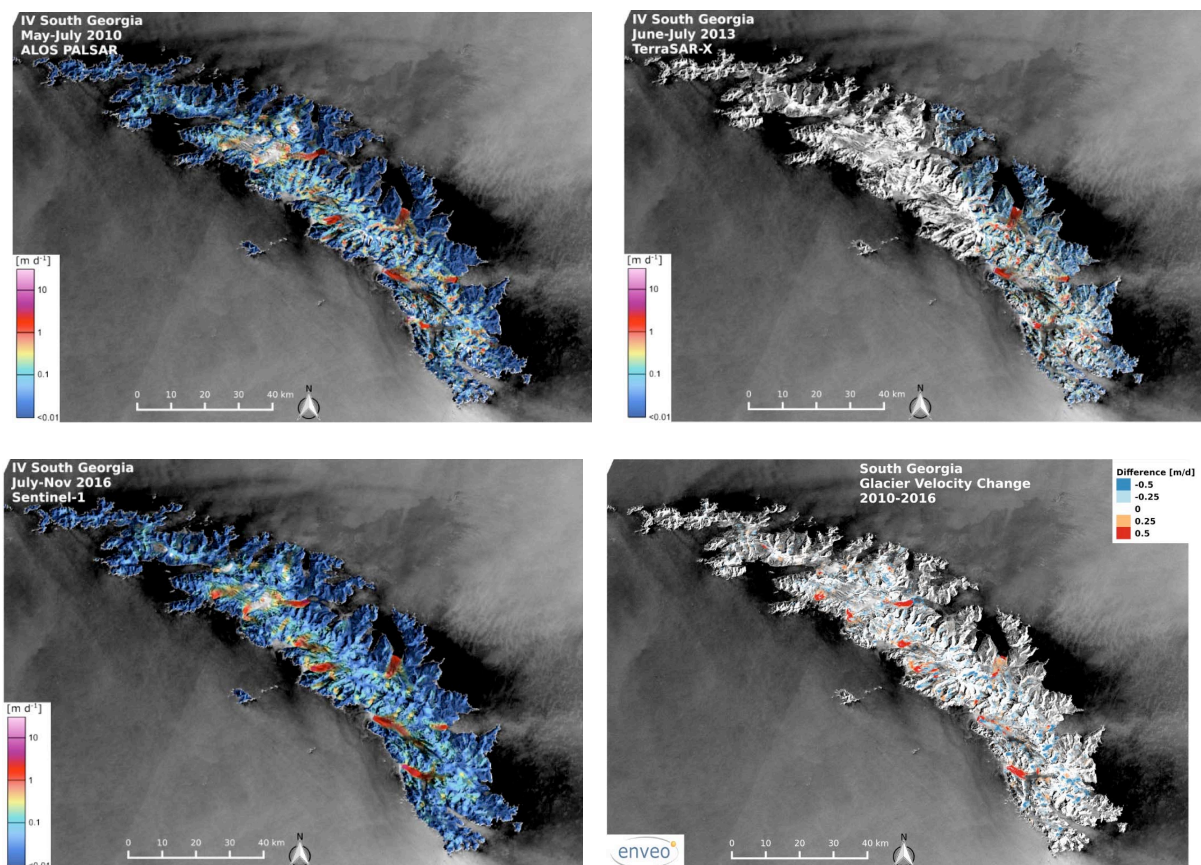


Figure 7.13: Velocity maps covering South Georgia (RGI region 19) derived from: ALOS PALSAR data acquired in May/July 2010 (top left), TerraSAR-X data acquired in June/July 2013 (top right), and Sentinel-1 data acquired in the period July 2016 to October 2016 (bottom left). The image in the bottom right panel shows the change in velocity between ALOS PALSAR (2010) and Sentinel-1 (2016). Background: S1 amplitude image.

7.7 Alexander Island, Antarctic Peninsula

ALOS PALSAR data acquired in 2010 were used to extend the velocity coverage for Alexander Island (Antarctic Peninsula, RGI region 19) back in time (Fig. 7.14). The IV map is derived applying feature tracking using ALOS PALSAR 46-day repeat image pairs acquired in FBS and FBD mode and is averaged over the period August 2010 to December 2010. The data set is posted at 200 m and provided in South Polar Stereographic projection (EPSG: 3031). For geocoding of the product, the Radarsat Antarctic Mapping Project DEM (RAMP DEM v2) is used and RGI 5.0 glacier outlines are used for validation. Based on the RGI the IV map successfully covers more than 70% of the island. The velocity field complements the Sentinel-1 derived IV product based on data acquired in the period Oct 2014 to Feb 2016.

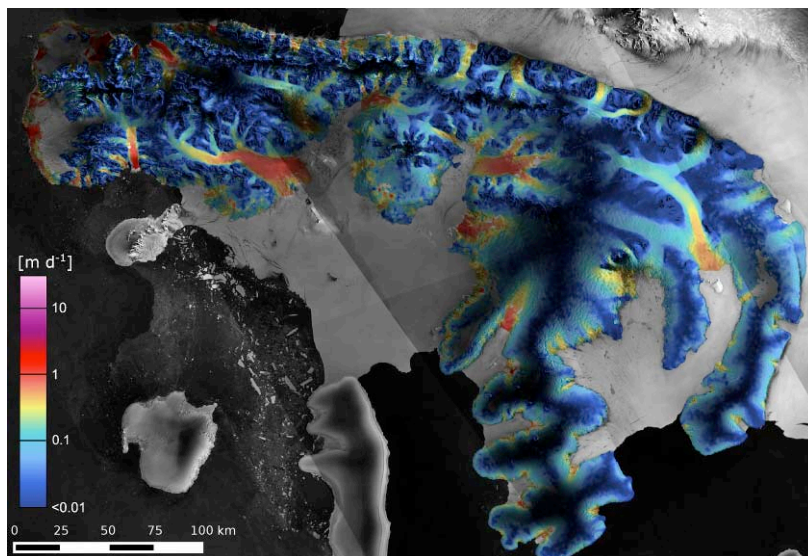
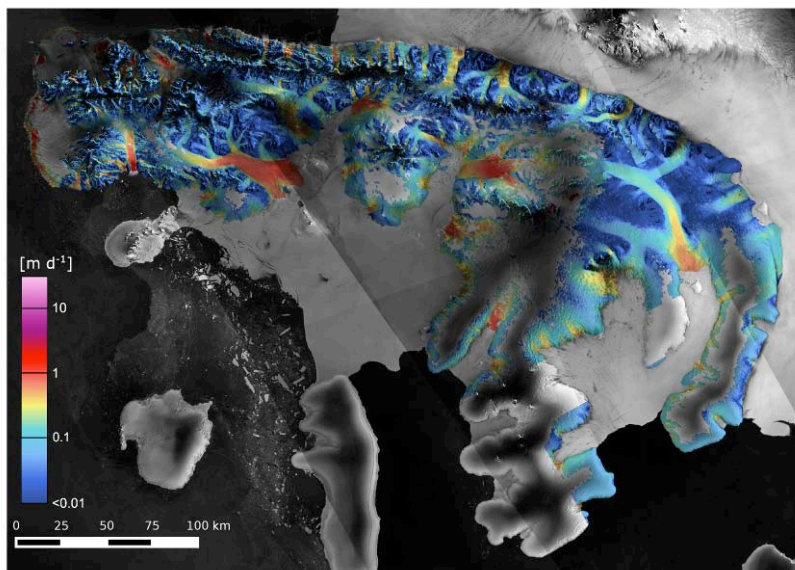


Figure 7.14: Velocity maps covering Alexander Island (Antarctic Peninsula, RGI region 19) derived from: ALOS PALSAR data acquired in August to December 2010 (top panel), and Sentinel-1 data acquired in the period Oct 2014 to Feb 2016 (bottom panel). Background: S1 amplitude image.

8. Phase 2 data production overview

Over the three years of Glaciers_cci Phase 2 a large number of datasets have been produced (Fig. 8.1). Many of them have been created to answer specific science questions and are thus also described in a journal publication (3, 6, 9, 10, 12, 13, 14, 16, 17, 19, 21). For several others a related journal publication is in preparation or foreseen (e.g. 1, 2, 4, 5, 7). Glacier outlines have been created from nearly all optical sensors (Landsat 5, 7, 8 and Sentinel 2) in nearly all regions of the world for different points in time (1985/2000/2015). Elevation changes have only been created for a few regions as the anticipated DEMs (TanDEM-X) were not available in time, but a wide range of DEMs and combinations with altimetry datasets have been applied and described. Velocity fields were created over large regions for two to three points in time or as dense time series over individual glaciers merging both optical and SAR data for optimal coverage.

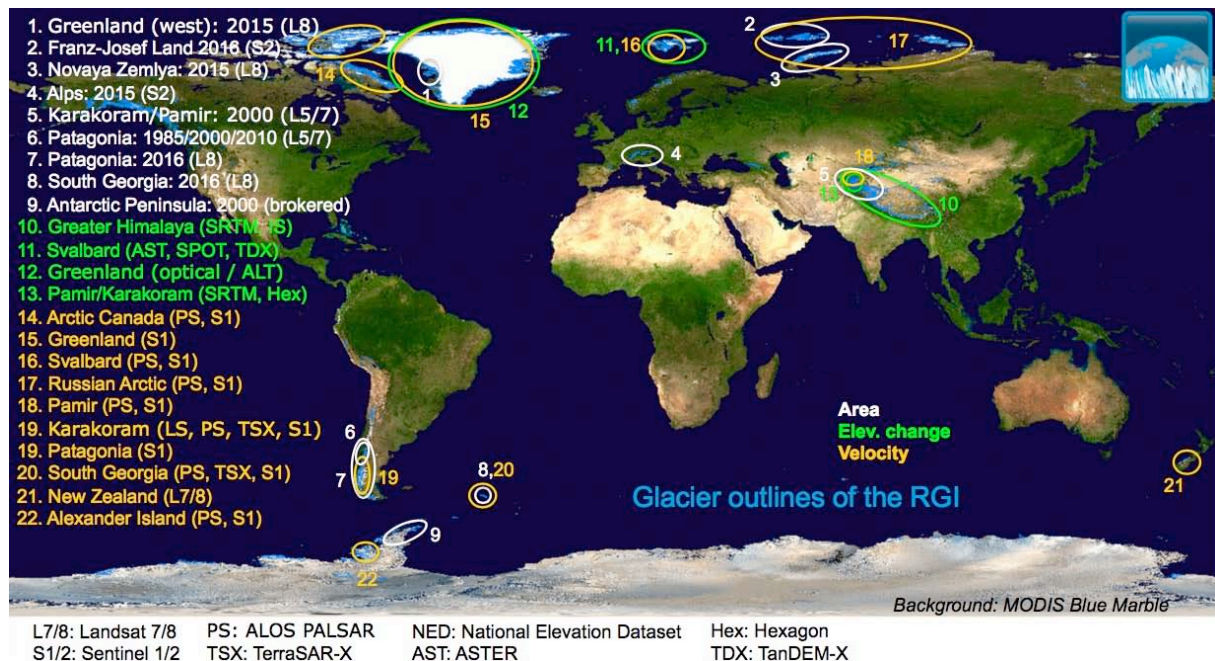


Fig. 8.1: Index map showing where the three products area (white), elevation change (green) and velocity (orange) have been produced. The listing to the left is also indicating years (for area only) and sensors or data sources for each region.

References

- Arendt, A. and 77 others (2015): Randolph Glacier Inventory [v5.0] - A dataset of global glacier outlines. Global Land Ice Measurements from Space, Boulder, CO. GLIMS Technical report, 63 pp. Online http://www.glims.org/RGI/00_rgi50_TechnicalNote.pdf
- Berthier, E., C. Larsen, W. Durkin, M. Willis, and M. Pritchard (2018): Brief communication: Unabated wastage of the Juneau and Stikine icefields (southeast Alaska) in the early 21st century, *The Cryosphere Discuss.*, <https://doi.org/10.5194/tc-2017-272>, in review.
- Citterio, M., F. Paul, A.P. Ahlstrøm, H.F. Jepsen and A. Weidick, A. (2009): Remote sensing of glacier change in West Greenland: accounting for the occurrence of surge-type glaciers. *Annals of Glaciology*, 50 (53), 70-80.
- Girod, L., C. Nuth, A. Käab, R. McNabb and O. Galland (2017): MMASTER: Improved ASTER DEMs for Elevation Change Monitoring. *Remote Sensing* 9(7), 704; doi:10.3390/rs9070704.
- Korona, J., E. Berthier, M. Bernard, F. Rémy and E. Thouvenot (2009): SPIRIT SPOT 5 stereoscopic survey of Polar Ice: Reference Images and Topographies during the fourth International Polar Year (2007–2009). *ISPRS Journal of Photogrammetry and Remote Sensing*, 64, 204-212.
- Paul, F., T. Strozzi, T. Schellenberger and A. Käab (2017): The 2015 surge of Hispar Glacier in the Karakoram. *Remote Sensing*, 9(9), 888; doi: 10.3390/rs9090888.
- Rastner, P., T. Strozzi and F. Paul (2017): Fusion of multi-source satellite data and DEMs to create a new glacier inventory for Novaya Zemlya. *Remote Sensing*, 9(11), 1122; doi: 10.3390/rs9111122.
- Strozzi, T., F. Paul, A. Wiesmann, T. Schellenberger and A. Käab (2017): Circum-Arctic changes in the flow of glaciers and ice caps from satellite SAR data between the 1990s and 2017. *Remote Sensing*, 9(9), 947; doi: 10.3390/rs9090947.

Abbreviations

ALT	Altimetry
ASTER	Advanced Spaceborne Thermal Emission and Reflection radiometer
CCI	Climate Change Initiative
CRDP	Climate Research Data Package
FBD	Fine Beam Double polarization
FBS	Fine Beam Single polarization
DEM	Digital Elevation Model
dDEM	differential DEM
GDEM	Global DEM
GLIMS	Global Land Ice Measurements from Space
ICESat	Ice, Cloud, and Elevation Satellite
InSAR	Interferometric SAR
IV	Ice Velocity
OLI	Operational Land Imager
PALSAR	Phased Array type L-band SAR
RGI	Randolph Glacier Inventory
S1, S2	Sentinel 1, Sentinel 2
SAR	Synthetic Aperture Radar
SPOT	System Pour l'Observation de la Terre
SRTM	Shuttle Radar Topography Mission
TM	Thematic Mapper